

Research Articles: Cellular/Molecular

Gamma Visual Stimulation Induces a Neuroimmune Signaling Profile Distinct from Acute Neuroinflammation

<https://doi.org/10.1523/JNEUROSCI.1511-19.2019>

Cite as: J. Neurosci 2019; 10.1523/JNEUROSCI.1511-19.2019

Received: 26 June 2019

Revised: 27 November 2019

Accepted: 2 December 2019

This Early Release article has been peer-reviewed and accepted, but has not been through the composition and copyediting processes. The final version may differ slightly in style or formatting and will contain links to any extended data.

Alerts: Sign up at www.jneurosci.org/alerts to receive customized email alerts when the fully formatted version of this article is published.

Copyright © 2019 Lu Zhangb and a,b et al.

This is an open-access article distributed under the terms of the Creative Commons Attribution 4.0 International license, which permits unrestricted use, distribution and reproduction in any medium provided that the original work is properly attributed.

Gamma Visual Stimulation Induces a Neuroimmune Signaling Profile Distinct from Acute Neuroinflammation

Abbreviated Title: Gamma stimulation induces neuroimmune signaling

Kristie M. Garza^{a,b}, Lu Zhang^b, Ben Borron^b, Levi B. Wood^{b,c,d,*,*}, Annabelle C. Singer^{b,c,*,*}

^aNeuroscience Graduate Program, Emory University, Atlanta, GA, 30033

^bWallace H. Coulter Department of Biomedical Engineering, Georgia Institute of Technology and Emory University, Atlanta, GA, 30332

^cParker H. Petit Institute for Bioengineering and Bioscience, Georgia Institute of Technology, Atlanta, GA, 30332

^dGeorge W. Woodruff School of Mechanical Engineering, Georgia Institute of Technology, Atlanta, GA, 30332

*Equally contributing corresponding authors

*Correspondence should be addressed to:

Levi Wood
315 Ferst Drive, Room 3303
Atlanta, GA 30332
levi.wood@me.gatech.edu

Annabelle Singer
313 Ferst Drive, Room 3105
Atlanta, GA 30332
asinger@gatech.edu

PAGES: 51

FIGURES, TABLES, MULTIMEDIA: 7 FIGURES, 1 MULTIMEDIA FILE

WORDS IN: ABSTRACT (248), INTRODUCTION (870), DISCUSSION (3,001)

CONFLICTS OF INTERESTS

A.C.S. owns shares in Cognito Therapeutics, which aims to develop gamma stimulation related products. Her conflicts of interest have been disclosed to and are managed by the Georgia Institute of Technology Office of Research Integrity Assurance.

ACKNOWLEDGEMENTS

We are grateful to members of the Singer and Wood laboratories for technical assistance and comments on the paper. This work was supported by Packard award in Science and Engineering (A.C.S), NIH R01-NS109226 (A.C.S), NIH R01-NS109226-01S1 (K.M.G), Friends and Alumni of Georgia Tech (A.C.S), Lane Family (A.C.S), startup funds from the Coulter Department of Biomedical Engineering (A.C.S) and the Woodruff School of Mechanical Engineering (L.B.W.) at the Georgia Institute of Technology.

ABSTRACT

1 Many neurodegenerative and neurological diseases are rooted in dysfunction of
2 the neuroimmune system, therefore, manipulating this system has strong therapeutic
3 potential. Prior work has shown that exposing mice to flickering lights at 40Hz drives
4 gamma frequency (~40Hz) neural activity and recruits microglia, the primary immune
5 cells of the brain, revealing a novel method to manipulate the neuroimmune system.
6 However, the biochemical signaling mechanisms between 40Hz neural activity and
7 immune recruitment remain unknown. Here, we exposed wildtype male mice to 5-60
8 minutes of 40Hz or control flicker and assessed cytokine and phospho-protein networks
9 known to play a role in immune function. We found that 40Hz flicker leads to increases
10 in expression of cytokines which promote microglial phagocytic states, such as IL-6 and
11 IL-4, and increased expression of microglial chemokines, such as M-CSF and MIG.
12 Interestingly, cytokine effects differed as a function of stimulation frequency, revealing a
13 range of neuroimmune effects of stimulation. To identify possible mechanisms
14 underlying cytokine expression, we quantified flicker's effect on intracellular signaling
15 pathways known to regulate cytokine levels. We found that 40Hz flicker upregulates
16 phospho-signaling within the NF κ B and MAPK pathways. While cytokine expression
17 increased after 1 hour of 40Hz flicker stimulation, protein phosphorylation in the NF κ B
18 pathway was upregulated within minutes. Importantly, the cytokine expression profile
19 induced by 40Hz flicker was different from cytokine changes in response to acute
20 neuroinflammation induced by lipopolysaccharides. These results are the first, to our
21 knowledge, to show how visual stimulation rapidly induces critical neuroimmune
22 signaling in healthy animals.

23

24 **Significance statement:** Prior work has shown that exposing mice to lights flickering at
25 40Hz induces neural spiking activity at 40Hz (within the gamma frequency) and recruits
26 microglia, the primary immune cells of the brain. However, the immediate effect of 40Hz
27 flicker on neuroimmune biochemical signaling was unknown. We found that 40Hz flicker
28 leads to significant increases in the expression of cytokines, key immune signals known
29 to recruit microglia. Furthermore, we found that 40Hz flicker rapidly changes
30 phosphorylation of proteins in the NF κ B and MAPK pathways, both known to regulate
31 cytokine expression. Our findings are the first to delineate a specific rapid immune
32 signaling response following 40Hz visual stimulation, highlighting both the unique nature
33 and therapeutic potential of this treatment.

34 INTRODUCTION

35 Interactions between the brain and immune system play critical roles in
36 neurological and neuropsychiatric disorders (Calsolaro and Edison, 2016; Wohleb et al.,
37 2016) . The neuroimmune system, including glial cells and immune signaling molecules,
38 offers a unique target to treat disease and improve brain health. However, little is known
39 about how to non-pharmacologically manipulate the brain's immune system. Recent
40 research has shown that exogenously stimulating neural electrical activity at gamma
41 frequency (30-50Hz), through sensory stimulation, promotes microglial activity, a
42 component of the neuroimmune system, and decreases amyloid-beta ($A\beta$), one of the
43 key proteins that build up in Alzheimer's disease (AD) (Iaccarino et al., 2016; Adaikkan
44 et al., 2019). While this recent research shows that neural electrical activity manipulates
45 a component of the neuroimmune system and has therapeutic implications, a broader
46 understanding of how exogenous stimulation of neural activity affects neuroimmune
47 function is required. Indeed, the immediate effects of exogenous gamma stimulation on
48 biochemical signals that control immune function in the brain are unknown. While the
49 previous literature in this area has focused on Alzheimer's disease pathology, it is
50 important to understand these basic biological interactions between neural activity and
51 immune function in healthy animals outside the context of AD. Furthermore, while 40Hz
52 visual stimulation is hypothesized to recruit the immune system, the effects of different
53 frequencies of visual stimulation on immune signaling remains unknown. Determining
54 how different frequencies of visual stimulation affect the immune system in the brain will
55 enable new strategies to manipulate brain function.

56 Cytokines, extracellular soluble signaling proteins of the immune system, are a
57 main communication signal between neurons and immune cells (Hanisch, 2002; Prieto
58 and Cotman, 2017). Chemotactic cytokines, or chemokines, are responsible for
59 attracting immune cells to a site of injury and pro- and anti-inflammatory cytokines
60 promote or reduce inflammation, respectively. While molecular signaling between
61 neurons and microglia has been largely attributed to neuronal expression of the
62 cytokine fractalkine (CX3CL1), which attenuates microglial over-activation (Sheridan
63 and Murphy, 2013), many other cytokines may play a role in signaling between neurons
64 and microglia. For example, glial-derived TNF- α is necessary for proper neuronal
65 synaptic scaling and is also a modulator of microglia neuronal phagocytosis (Stellwagen
66 and Malenka, 2006; Goshen et al., 2007; Neniskyte et al., 2014). Besides regulating
67 microglial activation and recruitment, cytokines are also involved in diverse neuronal
68 and synaptic functions. Still, little is known about how neuronal electrical activity affects
69 cytokine expression.

70 Cytokine expression and its effects on immune function are regulated by
71 intracellular signaling, such as the nuclear factor kappa-light-chain-enhancer of
72 activated B cells (NF κ B) and the mitogen activated protein kinase (MAPK)
73 immunomodulatory pathways. These pathways are activated through the subsequent
74 phosphorylation of proteins in a cascade, or phospho-signaling, and they culminate in
75 the activation of transcription factors, which regulate cytokine transcription, expression,
76 and release from the cell. Both the NF κ B and MAPK immunomodulatory pathways
77 strongly regulate expression of diverse cytokines involved in immune responses, like
78 microglial activation and recruitment (e.g., M-CSF, MCP-1) (Hommes et al., 2003;

79 Cloutier et al., 2007; Liu et al., 2017). These pathways also control expression of
80 neurotrophic and synaptotrophic factors and are involved in mechanisms of learning
81 and memory (Sweatt, 2001; Kaltschmidt et al., 2006; Mattson and Meffert, 2006; Chen
82 et al., 2017). Recent studies have shown 40Hz flicker changes protein phosphorylation
83 patterns after weeks of exposure compared to no stimulation, but the immediate effect
84 of flicker on protein phosphorylation in general and the immediate effects of flicker on
85 these two key phospho-protein pathways is still unknown (Adaikkan et al., 2019).

86 In the present study, we determined how 40Hz visual stimulation affects
87 expression of key cytokines involved in the brain's immune response, synaptic plasticity,
88 and neuronal health. Furthermore, since cytokine expression is regulated by
89 intracellular signaling, we assessed if NF κ B and MAPK phospho-signaling changes
90 prior to increases in cytokine expression in mice exposed to 40Hz visual stimulation
91 compared to control visual stimuli. We tested this by exposing mice to varying durations
92 of light emitting diode (LED) light strips flickering at 40Hz, which is known to induce
93 gamma neuronal activity, as well as several control conditions (Gray et al., 1989;
94 Iaccarino et al., 2016; Singer et al., 2018; Adaikkan et al., 2019). Our analysis showed
95 that 1 hour of 40Hz flicker stimulation induces phospho-signaling within the NF κ B and
96 MAPK pathways (~15-60 minutes) and protein expression of diverse cytokines.
97 Interestingly, 20Hz flicker, random flicker, and constant light each induced unique
98 cytokine expression profiles, revealing that different frequencies of visual stimulation
99 induce unique immune signaling patterns. We then determined if the cytokine response
100 after 40Hz flicker differed from that due to a model of acute inflammation induced by
101 lipopolysaccharides (LPS) administration. We found that the cytokine profile of acute

102 inflammation due to LPS administration was distinct from the cytokine response to 40Hz
103 flicker. These results show that 40Hz flicker induces NF κ B phospho-signaling followed
104 by MAPK phospho-signaling and increased cytokine expression distinct from
105 inflammation. Importantly, the cytokines assessed here, as well as the NF κ B and MAPK
106 pathways, play key roles in many different cellular functions. Furthermore, different
107 frequencies of stimulation induced unique cytokine expression patterns. Thus, our
108 results suggest that stimulation of different patterns of activity may be used to regulate
109 expression of genes that promote neuronal health, synaptic plasticity, and healthy
110 immune activity.

111

112 **MATERIALS AND METHODS**

113 **Animals**

114 All animal work was approved by The Georgia Tech Institutional Animal Care and
115 Use Committee. Adult (2-3 month old) male C57BL/6J mice were purchased from The
116 Jackson Laboratory. Mice were pair housed upon arrival and allowed to acclimate to the
117 environment for at least 5 days before being handled.

118 For all animals, food and water were provided *ad libitum*. For three days before
119 the experiment, mice were single-housed and briefly handled (about 1 minute per
120 mouse). All experiments were performed during the light cycle and began between 8
121 and 9 AM. For experiments with flicker durations of less than 1 hour, animals
122 undergoing the same stimulation condition were interspersed with animals undergoing
123 different conditions, to ensure circadian rhythms did not impact results. For experiments

124 with duration of flicker exposure at 1 hour, we conducted multiple experiments, at
125 different times of day, with varying order of stimulus presentation, to ensure results
126 remained consistent (data not shown).

127

128 **Visual Stimulation Exposure**

129 To habituate and reduce visual stimulation, mice were placed in a dark room in
130 the laboratory, for at least one hour, before beginning each experiment. To commence
131 the experiment, mice were transferred from their home cage to a similar cage without
132 bedding, termed a flicker cage. The flicker cage was covered in dark material on all but
133 one side, which was clear and faced a strip of LED lights. Animals remained in the dark
134 room, where they were exposed to either LED lights flashing at 40Hz frequency (12.5ms
135 light on, 12.5ms light off), 20Hz frequency (25ms light on, 25ms light off), a random
136 frequency which averaged at 40Hz (12.5ms light on, variable duration light off), or
137 constant light on stimulation, utilizing a dimmer to ensure the same total lux (about 150
138 lx) as 40Hz light flicker (**Video 1**)(Singer et al., 2018). These conditions allowed us to
139 control for light stimulation (light), light stimulation flashes (random), and frequency
140 specific stimulation (20Hz). Animals were exposed to visual stimulation for 5 minutes,
141 15 minutes, or 1 hour.

142 Immediately after stimulation exposure, mice were anesthetized with isoflurane,
143 and within 3 minutes mice were decapitated and brains were removed. The left
144 hemisphere's visual cortex was micro-dissected, placed in an Eppendorf tube, and flash
145 frozen using liquid nitrogen.

146 Cytokine analysis was conducted using six animals per group. Phospho-protein
147 experiments were conducted and combined across several cohorts of animals, utilizing
148 a total of 72 animals. More animals were utilized for experiments examining 5 minutes
149 of stimulation due to concern that initial signals at this time point may be transient and
150 hard to detect.

151

152 **Lipopolysaccharides (LPS) Stimulation**

153 Animals were intraperitoneal (i.p.) injected with 5mg/kg LPS (n=6), diluted in
154 saline (Sigma lot #039M-4004V) or saline (veh) (n=5). 3 hours after injection, mice were
155 anesthetized with isoflurane, and within 3 minutes mice were decapitated and brains
156 were removed. The left hemisphere's visual cortex was micro-dissected, placed in an
157 Eppendorf tube, and flash frozen using liquid nitrogen. Cytokine analysis was conducted
158 as described below.

159

160 **Cytokine and phospho-protein assays**

161 For signaling and cytokine analysis, the visual cortex was thawed on ice and
162 lysed using Bio-Plex lysis buffer (Bio-Rad). After lysing, samples were centrifuged at 4C
163 for 10 minutes at 13,000 RPM. Protein concentrations in each sample were determined
164 using a Pierce BCA Protein Assay (Thermo Fisher). Total protein concentrations were
165 normalized in each sample using Bio-Plex lysis buffer (Bio-Rad). For MAPK and NF κ B
166 pathway analysis, 1.5 μ g of total protein was loaded, and 6 μ g was loaded for cytokine
167 analysis. Preliminary experiments determined these protein concentrations fell within
168 the linear range of bead fluorescent intensity versus protein concentration for detectable

169 analysis. Multiplexed phospho-protein analysis was conducted by adapting the
170 protocols provided for the Milliplex MAP MAPK/SAPK Signaling Magnetic Bead 10-Plex
171 (p-ATF2, p-Erk, p-HSP27*, p-JNK, p-c-Jun, p-MEK1, p-MSK1, p-p38*, p-p53*) kit and
172 the Milliplex MAP NF κ B Signaling Magnetic Bead 6-Plex Kit(c-Myc*, p-FADD, p-I κ B α *,
173 p-IKK α/β , p-NF κ B, TNFR1). Cytokine analysis was conducted by adapting protocols
174 provided for the Milliplex Mouse MAP Mouse Cytokine/Chemokine Magnetic Bead
175 Panel 32-Plex Kit (Eotaxin, G-CSF, GM-CSF, IFN- γ , IL-1 α , IL-1 β , IL-2, IL-3, IL-4, IL-5,
176 IL-6, IL-7, IL-9, IL-10, IL-12p40, IL-12p70, IL-13, IL-15, IL-17, IP-10, KC, LIF, LIX, MCP-
177 1, M-CSF, MIG, MIP-1 α , MIP-1 β , MIP-2, RANTES, TNF- α , and VEGF). All kits were
178 read on a MAGPX system (Luminex, Austin, TX). Asterisks denote analytes that did not
179 fall within the linear range and were therefore excluded from our analysis.

180

181 **Partial least squares discriminant analysis**

182 Data was z-scored before analysis. A partial least squares discriminant analysis
183 (PLSDA) was performed in MATLAB (Mathworks) using the algorithm by Cleiton Nunes
184 (Mathworks File Exchange) (Eriksson, L.; Byrne, T.; Johansson, E.; Trygg, J.; Vikström,
185 2006). To identify latent variables (LVs) that best separated conditions, an orthogonal
186 rotation in the plane of the first two latent variables (LV1-LV2 plane) was performed.
187 Error bars for LV1 figures represent the mean and standard deviations after iteratively
188 excluding single samples (a leave-one-out cross validation), one at a time, and
189 recalculating the PLSDA 1000 times.

190 To test different flicker conditions and durations, phospho-protein experiments
191 were performed over several cohorts and samples were normalized by removing batch

192 effects. We performed a batch effects analysis (limma package in R v 3.5.2) to remove
193 any between-experiment-variability before conducting the PLSDA. Outliers were
194 removed by performing a principle component analysis on the data and iteratively
195 removed data points which fell outside of a 99.5% confidence ellipse (mahalanobisQC
196 in R v 3.5.2).

197

198 **Animal behavior assays**

199 To analyze animal behavior, mice were placed in a polycarbonate cage (210
200 x375 x 480mm), covered on all sides but one with 100% polyester black material
201 (similar to cage in visual flicker experimental protocol cage described above, but larger
202 and without cage top). In order to record the mice in the dark, an infrared (IR) light was
203 placed above the cage. To record mice, without the flicker stimulation affecting
204 behavior tracking, a Basler Ace monochrome IR-sensitive camera with Gigabit Ethernet
205 interface with attached IR-only filter was used for recording. Ethernet connection from
206 the camera to the computer allowed for Ethovision to record and analyze the
207 experiment in real time.

208 Three days before recording, mice were handled as described in flicker
209 experiment section above. On the third handling day, each mouse was placed in the
210 behavior cage to habituate for five minutes. On the fourth day, each mouse was
211 recorded individually for an hour and five minutes while receiving one of four flicker
212 treatments (40Hz, 20Hz, random, light). Behavior assays were conducted using a total
213 of six animals, with a within-subjects design. Each mouse received each treatment

214 separated by 1 day in a randomized order. Experimenter was blinded to treatment type
215 during experiment and analysis.

216 Ethovision XT version 14.0 was used to track and analyze behavior. First, the
217 arena was defined, and a zone group defined which split the bottom of the cage in to
218 two halves, front and back. A second zone group defined as center consisted of half of
219 the total area in the center of the cage. Detection settings were made using Ethovision's
220 automatic detection function and were adjusted after preliminary analysis. Automated
221 video analysis recorded the animals' center point and all recordings were checked and
222 manually corrected through software interpolation for any time points in which the
223 mouse could not be automatically detected. Activity level was designated as active or
224 inactive with inactive indicating freezing. Inactivity was determined to be less than
225 0.01% of the total arena having activity and lasting for a duration longer than half a
226 second. Data for each variable was exported and analyzed using GraphPad. A one-
227 way analysis of variance (ANOVA) was conducted to assess differences between
228 groups for each variable of interest.

229

230 **Experimental design and statistical analysis**

231 Animals were randomly assigned to flicker exposure groups and experimenters
232 were blind to flicker exposure conditions during analysis for all experiments. Sample
233 sizes were determined on preliminary data with a 0.80 power and alpha of 0.05, and
234 samples sizes were adjusted based on high variability. Control groups (20 Hz, random,
235 and light) were based on prior experiments and preliminary data.

236 For multi-plex analysis, either a one-way ANOVA (more than two groups) or two-
237 tailed unpaired t-test (two groups) was used to determine if there was a significant LV1
238 separation between groups. The top correlated cytokines and/or phospho-proteins on
239 the LV1 were isolated and an ANOVA or two-tailed unpaired t-test was performed using
240 GraphPad Prism 8 (GraphPad Software, La Jolla, CA) to determine statistical
241 significance between groups. These tests were followed by a post-hoc Dunnett's
242 multiple comparisons test to determine differences between specific groups or a
243 Tuckey's multiple comparisons test to compare differences in phosphorylation levels
244 across time. Levels of significance were set to * $p < 0.05$, ** $p < 0.01$, **** $p < 0.001$.

245 To further confirm significant differences between groups using PLSDA, a
246 permutation analysis was conducted, which randomly assigned animals into
247 experimental groups and ran the PLSDA based on these shuffled values 1000 times
248 (Golland et al., 2010). For each test, true group assignment showed $p_{\text{permute}} < 0.05$
249 compared to the randomly permuted distribution, further confirming the validity of our
250 data.

251 For analyzing changes in animal behavior, a one-way repeated measures
252 analysis of variance (RM-ANOVA) was to compare results between different stimulation
253 types.

254 For comparing between LPS-treated and 40Hz-stimulated animals, each group
255 was normalized to control. Specifically each cytokine level in each animal was divided
256 by the mean cytokine level in the related control group (vehicle for LPS and random for
257 40Hz). Multiple t-tests were then conducted to compare each stimulation to its control;
258 multiple comparisons were corrected using the Holm-Sidak method.

259

260 **Code accessibility**

261 Data was analyzed using custom code that is available upon request.

262

263 **RESULTS**264 **40Hz flicker induces increased cytokine profile**

265 Given previous findings showing that exposing mice to 40Hz light flicker leads to
266 morphological changes in microglia, we speculated that 40Hz flicker affects
267 neuroimmune signaling. Specifically, since cytokines are key regulators of immune
268 activity in the brain, we hypothesized that 40Hz light flicker promotes cytokine
269 expression in the visual cortex. To test this, we exposed animals to 1 hour of 40Hz
270 flickering light, light flickering at a random interval averaging at 40Hz (random), 20Hz
271 flickering light (20Hz), and constant light (light)(**Fig. 1A, Video1**). After visual stimulation,
272 mice were euthanized, and the visual cortex was rapidly (<3min) micro-dissected and
273 flash frozen. Using a Luminex multi-plexed immunoassay we quantified expression
274 levels of thirty-two cytokine proteins in the visual cortex (**Fig. 1B**). To account for the
275 multi-dimensional nature of the data, we used a PLSDA to identify profiles of cytokines
276 that distinguished the effects of 40Hz stimulation from the control groups (**Fig. 1C**)
277 (Eriksson, L.; Byrne, T.; Johansson, E.; Trygg, J.; Vikström, 2006).

278 We observed overall higher cytokine expression levels across animals exposed
279 to 40Hz flicker compared to other groups. PLSDA identified a latent variable 1 (LV1),
280 consisting of a weighted linear combination of cytokines, as being most upregulated in

281 40Hz (higher LV1 scores) or from all control conditions ((negative) (lower LV1 scores),
282 **Fig. 1D**). LV1 best separated 40Hz from all control groups (**Fig. 1C, Fig.1D**). LV1
283 scores differed significantly between groups confirming the groups were statistically
284 separate, specifically, 40Hz flicker versus light and 20Hz stimulation were best
285 separated ($F(3, 20) = 5.855$, $p=0.0049$, one-way ANOVA) (**Fig. 1E**). LV2 significantly
286 separated control groups from each other ($F(3,20)=21.77$, $p<0.0001$, **Fig.1C, Fig. 2B**).

287 The top four identified by the PLSDA to contribute to differences between groups
288 were M-CSF, IL-6, MIG, and IL-4 (**Fig. 1F**). Of these top upregulated cytokines, IL-6 and
289 MIG were significantly different between groups when each one was analyzed
290 individually (IL-6: $F(3,20)=3.775$, $p=0.0269$; MIG: $F(3,20)=4.532$, $p=0.0140$, one-way
291 ANOVA) (**Fig. 1F**). We found IL-6 had significantly higher expression in 40Hz than 20Hz
292 flicker and light; and MIG had significantly higher expression in 40Hz than 20Hz flicker
293 (IL-6: 40Hz versus 20Hz: mean difference =1.917, adjusted $p=0.0452$; IL-6: 40Hz
294 versus light: mean difference= 2.33, adjusted $p=0.0135$; MIG: 40Hz versus 20Hz: mean
295 difference =2.083, adjusted $p=0.0123$, Dunnett's test). M-CSF expression was higher in
296 40Hz flicker than light exposed animals (mean difference = 1.750, adjusted $p=0.0360$.
297 Dunnett's test). We found no significant differences in IL-4 between groups although
298 expression levels trended towards being higher in 40Hz flicker animals
299 ($F(3,20)=2.051$, $p=0.1391$, one-way ANOVA). Based on observed differences between
300 groups in a heatmap of these cytokines (**Fig.1B**), we ran additional analysis on a subset
301 of cytokines and found significant differences in IL-12p70, IL-1 β , IFN- γ , GM-CSF, IL-7
302 between 40Hz flicker and control conditions (see **Fig. 1G**). These findings show that 1

303 hour of 40Hz flicker drives a significant neuroimmune signaling response, and this
304 response is distinct from other flicker frequencies or exposure to constant light.

305 Interestingly, while animals exposed to 40Hz flicker showed a higher cytokine
306 expression profile, we also observed distinct cytokine expression profiles for random,
307 20Hz, and light stimulation conditions (**Fig.1B, Fig. 2C**). Indeed, our analysis revealed a
308 second latent variable (LV2), which best separated these three control groups (**Fig. 1C,**
309 **Fig.2A**). Quantification of these effects showed constant light leads to an upregulation
310 of a subset of cytokines, unique from those upregulated by 40Hz flicker. For example,
311 when analyzed individually, IL-2, VEGF, IL-9, IL-1 α , and IL-13 all showed significant
312 differences in expression levels between groups, with higher upregulation after light
313 exposure than at least one other group (IL-2: $F(3,20)=9.366, p=0.0005$; VEGF:
314 $F(3,20)=6.790, p=0.0024$; IL-9: $F(3,20)=4.076, p=0.0207$; IL-1 α : $F(3,20)=4.399, p=0.0157$;
315 IL-13: $F(3,20)=3.802, p=0.0263$; one-way ANOVA, Dunnett's multiple comparisons
316 method was used to control for 3 comparisons, **Fig. 2E-2I**) In contrast, random
317 stimulation uniquely upregulated IL-10 across all samples, when compared to other
318 stimulation types ($F(3, 20) =27.29, p<.0001$, **Fig. 2D**) These results highlight that while
319 40Hz flicker modulated cytokine activity, 20Hz, random, and light exposure also led to
320 distinct cytokine activity.

321

322 **40Hz flicker induces NF κ B and MAPK signaling**

323 Cytokine expression is regulated by several canonical intracellular phospho-
324 signaling pathways, including the NF κ B and MAPK pathways. Thus, to gain better
325 insight into intracellular signaling changes that underlie changes in cytokine expression

326 after visual stimulation, we examined how 40Hz flicker impacted these two phospho-
327 protein pathways. Because phospho-signaling is usually transient, we examined this
328 signaling after 5, 15, and 60 minutes of 40Hz and random flicker (Janes et al., 2005).
329 We focused on random flicker as our control group for this comparison specifically
330 because it controls for the average number of times the lights turn on and off, the
331 percent of time the light is on, and the frequency of light presentation without inducing
332 periodic neural activity (Iaccarino et al., 2016; Singer et al., 2018; Adaikkan et al., 2019).
333 As with cytokine experiments, immediately following flicker exposure, mice were
334 euthanized, and visual cortex was rapidly micro-dissected. We used Luminex assays
335 and PLSDA to quantify differences in the NF κ B and MAPK phospho-protein pathways in
336 40Hz versus random flicker exposure animals after different durations of flicker (**Fig. 3,**
337 **4**).

338 We found phospho-signaling in the NF κ B pathway was significantly upregulated
339 after 15 minutes, but not 5 or 60 minutes, of 40Hz versus random flicker. Experiments
340 were performed across several cohorts and animals were removed based on an outlier
341 analysis; data was z-scored according to batch-corrected data (see **Methods**). Our
342 analysis revealed a trend of increased phosphorylation after 5 minutes of flicker, driven
343 specifically by increases in TNFR1 and pIKK α/β , but 40Hz and random groups were not
344 significantly different ($t(21) = 2.056$, $p = 0.0525$, unpaired t-test, **Fig. 3B, 3E**). After 15
345 minutes of flicker exposure, NF κ B phosphorylation significantly differed between groups
346 as indicated by significant separation of NF κ B LV1 scores ($t(16) = 4.456$,
347 $p = 0.0004$, unpaired t-test, **Fig. 3C, 3F**). At 60 minutes, there was no significant difference
348 between groups but phosphorylation of NF κ B proteins appeared lower in 40Hz than

349 random groups ($t(8) = 1.415$, $p = 0.1948$, unpaired t-test, **Fig. 3D, 3G**). These results show
350 that 40Hz flicker transiently upregulates the NF κ B pathway after approximately 5 to 15
351 minutes and this difference in upregulation is no longer detectable after 60 minutes of
352 flicker.

353 We found that MAPK phosphorylation patterns were similar to those of NF κ B but
354 with different kinetics. MAPK phospho-signaling was significantly different between
355 40Hz and random groups after 60 minutes of flicker but not after 5 or 15 minutes.
356 Phosphorylation of MAPK proteins following 5 minutes of 40Hz flicker did not
357 significantly differ from random stimulation as indicated by no significant LV1 separation
358 ($t(32) = 1.870$, $p = 0.0707$, unpaired t-test) (**Fig. 4B, 4E**). While phosphorylation of MAPK
359 proteins also did not significantly differ following 15 minutes of 40Hz or random flicker
360 ($t(8.582) = 1.99$, $p = 0.2624$, welch corrected unpaired t-test), the heatmap of phospho-
361 protein levels showed a trend for more phosphorylated MAPK proteins in 40Hz than
362 random group (**Fig. 4C, 4F**). MAPK phospho-signaling did significantly differ between
363 40Hz and random stimulation following 60 minutes of flicker exposure, as revealed by
364 significantly separated LV1 scores ($t(10) = 3.709$, $p = 0.004$, unpaired t-test, **Fig. 4D, 4G**).
365 This effect was mostly driven by differences in phosphorylated MSK1, and MEK1 (**Fig.**
366 **4J**). These results show that 40Hz flicker upregulates the MAPK pathway after
367 approximately 60 minutes.

368

369 **Correlations between phosphorylation of proteins increases after minutes**
370 **of 40Hz flicker**

371 Because phospho-signaling is transient, another way of assessing activity in
372 these pathways is to measure coordinated phosphorylation among proteins. We thus
373 hypothesized that activation of these pathways would lead to coordinated phospho-
374 protein levels at time points prior to our observed increases in cytokine expression.
375 Therefore, we examined how coordination both within and between NF κ B and MAPK
376 networks changed over the course of 40Hz flicker exposure. In order to do so, we
377 utilized variability across animals and investigated protein co-variation across animals
378 by calculating the correlation coefficients of each protein pair from NF κ B and MAPK
379 pathways after 5, 15 and 60 minutes of 40Hz flicker stimulation (Eisen et al., 1998;
380 Kanonidis et al., 2016) (**Fig. 5**). In other words, this analysis revealed protein
381 phosphorylation levels that significantly increased or decreased together across animals
382 (**Fig. 5**, $q < 0.1$, false discover rate correction for 135 comparisons, Pearson correlation
383 test).

384 Over the time points assessed, we found the number of significant correlations
385 between proteins within each pathway was highest after 15 minutes of 40Hz flicker.
386 After 5 minutes of 40Hz flicker, five proteins were significantly correlated within the
387 NF κ B pathway and four within the MAPK pathway (**Fig. 5A**). After 15 minutes of 40Hz
388 flicker, more protein correlations were found: 6 significant correlations in the NF κ B
389 pathway and 10 significant correlations in the MAPK pathway (**Fig. 5B**). Interestingly,
390 the proteins that were significantly correlated after 15 but not 5 minutes of flicker were
391 farther downstream in the MAPK pathway: pERK1/2, pMSK1, pATF-2, and pSTAT1

392 (Fig. 4A). After 60 minutes of 40Hz flicker, only 3 significant correlations were found in
393 both pathways (Fig. 5C). Of note, all significant correlations were within and not across
394 NF κ B and MAPK pathways in all time points assessed.

395

396 **Animal behavior is similar across flicker conditions**

397 Given our findings indicating cytokine and phospho-protein upregulation induced
398 by 40Hz flicker, we sought to determine if behavioral differences during flicker could
399 explain these results. We assessed both overall activity levels, measured as percent
400 time active and total distance traveled, as well as exploratory versus anxiety-like
401 behavior, assess by the percent of time animals spent in the center of the environment
402 versus along the walls (perimeter). More anxious animals stay close to the walls of an
403 enclosure. We recorded mice during 1 hour of either 40Hz flicker, random flicker, 20Hz
404 flicker, or light and tracked mouse movement (Fig. 6A). Our results revealed no
405 significant differences between different flicker conditions in the amount of time spent in
406 the center versus the perimeter of the enclosure, time spent active instead of freezing,
407 time spent in the front (near the light source) versus the back half of the enclosure, and
408 total distance traveled (Center versus perimeter: Fig. 6B, $F(3,15)=0.8754$, $p=0.4757$,
409 RM-ANOVA; Activity: (Fig. 6C, $F(3,15)=0.9304$, $p=0.4502$, RM-ANOVA; Front versus
410 Back: Fig.6D, $F(3,15)=0.1727$, $p=0.9132$, RM-ANOVA; Distance: Fig.6E,
411 $F(3,14)=0.3392$, $p=0.7973$, RM-ANOVA). These results show different visual stimulation
412 conditions including different frequencies of flicker, periodic or aperiodic flicker, or
413 constant or flickering light stimuli do not differentially affect animal behavior or induce an

414 anxiety-like phenotype. Thus, the molecular changes we found in response to different
415 visual stimulation conditions are not due to changes in animal behavior.

416

417 **40Hz flicker induces neuroimmune profile distinct from acute inflammation**

418 Next, we wondered how the cytokine profile in response to 40Hz flicker differed
419 from acute inflammation. Thus we assessed cytokine expression in the visual cortex of
420 animals intraperitoneally injected with lipopolysaccharides (LPS), a traditional, acute
421 model of inflammation (Gabellec et al., 1995; Qin et al., 2007; Meneses et al., 2018). As
422 in our flicker experiments, we characterized cytokine expression in visual cortex of mice
423 injected with LPS versus vehicle injection and separated these differences using a
424 PLSDA (**Fig. 7**). The latent variable that best separated LPS- and vehicle-injected
425 animals (LV1, *orange*) was most heavily weighted by expression of MIG, IP-10, IL-3,
426 and IL-17 (**Fig.7A**). The profile of cytokines weights that separated LPS from vehicle
427 injected animals (LV1, *orange*) differed from the profile that separated 40Hz versus
428 random stimulation exposed animals (LV1, *blue*, **Fig. 7A**). These results show that
429 40Hz flicker and LPS stimulation lead to distinct immune profiles.

430 We further analyzed the differences between LPS and 40Hz flicker by comparing
431 individual cytokines following LPS or 40Hz flicker relative to their controls. These
432 comparisons revealed that most cytokines differed between LPS and 40Hz flicker, both
433 in terms of whether or not each cytokine was modulated by the stimulus and in terms of
434 the magnitude of the response relative to control (**Fig. 7B,C,D**). For example, GM-CSF
435 and IL-2 significantly differed between animals exposed to 40Hz flicker versus random
436 stimulation but did not differ between animals injected with LPS or vehicle (*40Hz versus*

437 *random*: GM-CSF: $t(10)=3.114$, $p=0.011$; IL-2: $t(10)=3.613$, $p=0.0047$; *LPS versus*
438 *vehicle*: GM-CSF: $t(9)=1.646$, $p=0.134$; IL-2: $t(9)=0.167$, $p=0.871$) (**Fig. 7B**). In contrast,
439 G-CSF, KC, MIG, RANTES, IP-10, and IL-6 significantly differed between LPS and
440 vehicle but not between 40Hz and random (*LPS versus vehicle*: G-CSF: $t(9)=4.069$,
441 $p=0.003$; KC: $t(9)=3.883$, $p=0.004$; MIG: $t(9)=12.16$, $p<0.000001$; RANTES:
442 $t(9)=3.502$, $p=0.007$; IP-10: $t(9)=14.86$, $p<0.000001$; IL-6: $t(9)=3.107$, $p=0.013$; *40Hz*
443 *versus random*: G-CSF: $t(10)=1.661$, $p=0.128$; KC: $t(10)=0.450$, $p=0.662$, MIG:
444 $t(10)=0.2928$, $p=0.776$; RANTES: $t(10)=1.335$, $p=0.212$, IP-10: $t(10)=0.3421$, $p=0.739$; IL-
445 6: $t(10)=1.437$, $p=0.1813$) (Fig. 7C). Lastly, there was a subset of cytokines, IL-12p70,
446 Eotaxin, TNF- α , and MCP1, that significantly differed in both LPS versus vehicle and
447 40Hz versus random (*LPS versus vehicle*: IL-12p70: $t(9)=2.359$, $p=0.043$; Eotaxin:
448 $t(9)=2.710$, $p=0.024$; TNF- α : $t(9)=3.561$, $p=0.007$; MCP1: $t(9)=2.884$, $p=0.018$; *40Hz*
449 *versus random*: IL-12p70: $t(10)=3.729$, $p=0.004$; Eotaxin: $t(10)=2.318$, $p=0.043$; TNF- α :
450 $t(10)=3.512$, $p=0.006$; MCP1: $t(10)=2.785$, $p=0.019$) (Fig. 7D). For those cytokines that
451 significantly increased expression in response to both LPS and 40Hz stimulations
452 relative to controls, the scale of the difference between the two comparisons was
453 usually much larger when comparing LPS versus vehicle. For example, the difference in
454 expression of MCP1 was over 10 fold larger between LPS and vehicle than between
455 40Hz and random, though both differences were significant (**Fig. 7D**). Overall these
456 results show that acute inflammation via LPS and 40Hz flicker produce different immune
457 responses.

458

459 **DISCUSSION**

460 In this study, we utilized multiplexed immunoassays to profile expression of
461 cytokines and phospho-signaling within key pathways that regulate the brain's immune
462 response to different forms of visual stimulation. We found that 40Hz light flicker rapidly
463 and transiently stimulated phospho-signaling within the NF κ B pathway in mouse visual
464 cortex. NF κ B phospho-signaling was followed by increased phospho-signaling within
465 the MAPK pathway and increased expression of a diverse profile of cytokines involved
466 in microglial recruitment (e.g., M-CSF), neurotrophic properties (e.g., IL-6), and synaptic
467 plasticity (e.g., IL-1). Furthermore, we found distinct cytokine responses to different
468 visual stimuli, including 20 Hz flicker, random flicker, and constant light. These results
469 show that specific frequencies and patterns of visual stimulation lead to different
470 cytokine responses. Because these assays were performed in wild-type animals, the
471 results reveal that 40Hz flicker stimulation modulates immune function independent of
472 disease pathology. Thus, these findings suggest this approach could be applied to
473 many diseases that affect brain immune function. Importantly, we found that 40Hz
474 flicker induced a cytokine signature that differs from an LPS model of inflammation.
475 Together, our data show that visual flicker rapidly activates canonical intracellular
476 signaling pathways and induces a unique cytokine expression profile. Due to the
477 multifunctional nature of these pathways and the broad range of cytokines expressed,
478 the effects of visual flicker likely extend beyond neural immune activity to changes in
479 neuronal health, synaptic plasticity, and other functions.

480

481 **40Hz flicker-induces a unique cytokine profile in the visual cortex**

482 Because nothing is known about the effect of gamma oscillatory activity on
483 cytokine expression levels, we used a multi-plex approach to determine the global
484 impact of this activity on the brain's main immune signals. Our results establish that
485 40Hz flicker upregulated a combination of cytokines in the visual cortex resulting in a
486 neuroimmune profile distinct both from other types of flicker stimulation and from acute
487 inflammation induced by LPS. Interestingly, LV1 better separated 40Hz stimulation from

488 20Hz and light than from random stimulation. This point is reinforced by our finding that
489 the top LV1-contributing cytokines did not differ significantly between 40Hz and random
490 stimulation. However other cytokines, such as IFN- γ , IL-12p70, and GM-CSF, showed
491 significant differences between 40Hz and random stimulation (**Fig.1G**). Thus, random
492 stimulation leads to an immune profile with an overlap in expression of some cytokines
493 to that of 40Hz but distinct expression levels of other cytokines (**Fig. 2**). While random
494 stimulation does not induce gamma oscillations, randomized pulses of light slightly alter
495 neural activity in visual cortex over a much broader ranges of frequencies than gamma
496 frequency light flicker (Iaccarino*, Singer* et al., 2016). Therefore, random flicker has
497 some similar and some different effects on cytokines as 40Hz flicker but taken together
498 this still produces a distinct immune profile.

499 Random flicker, 20Hz flicker, and light stimulation each induce expression of
500 unique subsets of cytokines (**Fig. 2**). When comparing cytokine expression, LV1 best
501 separated 40Hz stimulation from the other controls. In contrast, LV2 best separated all
502 of the control groups from each other. Interestingly, while LV1 separated animals
503 stimulated with 20Hz and light stimulation from those stimulated with 40Hz visual flicker,
504 these groups were not as well separated by LV2. In fact, LV2 best separated animals
505 stimulated with random visual flicker from other groups. When examining individual
506 cytokines, plotted in Figure 2, there is a significant difference in expression of IL-10 and
507 RANTES between 40Hz and 20Hz flicker, and significant difference in expression of IL-
508 10, IL-15, and RANTES between 40Hz flicker and light. Together, these results
509 demonstrate that 40Hz stimulation leads to increased expression of the many cytokines

510 in the visual cortex compared to other conditions, but each of our control stimulations
511 produces its own unique profile of cytokine expression.

512

513 **40Hz flicker-induced cytokines have neuroprotective functions**

514 We found that 40Hz flicker is upregulating a unique combination of cytokines,
515 and we hypothesize that no one cytokine in particular is responsible for neuroprotective
516 function, but rather the combinatory profile is necessary. This effect would coincide with
517 what is known about gamma oscillations, that no one neuron is responsible for gamma
518 oscillations, but rather the combination of neuronal activity.

519 By focusing on the functions of the top five cytokines distinguishing 40Hz flicker
520 from all other groups M-CSF, IL-6, MIG, IL-4, and KC (also known as CXCL1), it
521 becomes apparent that each cytokine's unique immune function may contribute to an
522 overall neuroprotective effect (**Fig.1**)., M-CSF (encoded by *Csf1*) transforms microglia
523 morphologically and has been reported to enhance phagocytosis of amyloid beta (Imai
524 and Kohsaka, 2002; Mitrasinovic and Murphy, 2003). Furthermore, the primary receptor
525 for M-CSF, *Csf1r*, is primarily expressed by microglia in the brain (Elmore et al., 2014).
526 Thus, M-CSF may be responsible for previously observed morphological transformation
527 of microglia in 5XFAD mice (after 1 hour of 40Hz light flicker stimulation followed by 1
528 hour of no stimulation) because those microglial changes are associated with
529 engulfment (Iaccarino et al., 2016).

530 Interestingly, IL-6, the second top cytokine that increased following 1 hour of
531 40Hz flicker, is a pleiotropic cytokine with both protective and pathogenic effects. The
532 potential pathogenic effects of IL-6 include stimulating amyloid precursor protein

533 expression (Ringheim et al., 1998). In contrast, the neuroprotective effects of IL-6
534 include increasing synaptic density and inhibiting macrophage expression of TNF- α , a
535 cytokine known to have pro-inflammatory and neurotoxic properties (Decourt et al.,
536 2017). In our own work, increased expression of IL-6 was correlated with a resiliency to
537 Alzheimer's pathology; defined as human subjects with no neuronal loss or cognitive
538 impairment even in the presence of plaques and tangles associated with Alzheimer's
539 (Barroeta-Espar et al., 2019). IL-6 is also important for neural progenitor cell health as
540 IL-6 knockout significantly reduced neural progenitor cell density in multiple brain
541 regions (Bowen et al., 2011). Furthermore, IL-6 levels correlate with improved learning
542 and memory performance in both animals and humans (Baier et al., 2009; Donegan et
543 al., 2014; Wang et al., 2017).

544 The third flicker-upregulated cytokine, monokine induced by gamma interferon
545 (MIG), is a chemokine involved in microglial recruitment via its receptor, CXCR3
546 (Rappert, 2004). In brain endothelial cells *in vitro*, MIG is released in response to the
547 presence of other cytokines (Ghera et al., 2002). It is specifically responsible for
548 recruiting T-cells to the brain and responds to interferon gamma (IFN- γ), suggesting
549 MIG may be released to combat infection. Indeed, injecting mice with an anti-MIG
550 treatment leads to increased viral infection and pathology (Ure et al., 2005).

551 Finally, the fourth and fifth top cytokines, IL-4 and KC (CXCL1) signal to microglia
552 (Johnson et al., 2011; De Filippo et al., 2013; Fenn et al., 2014). IL-4 has been shown to
553 reprogram microglia to stimulate neurite outgrowth after spinal cord injury (Fenn et al.,
554 2014). In addition, AAV mediated over-expression of IL-4 in APP mice reduced A β
555 plaque load (Latta et al., 2015). KC (CXCL1) is a chemokine involved in recruiting

556 neutrophils, a type of white blood cell, signaling to microglia (Johnson et al., 2011; De
557 Filippo et al., 2013). Finally, KC signals to the receptor CXCR2, which is expressed on
558 microglia and has been reported to mediate microglial recruitment (Lee et al., 2012). In
559 total, our data show that 40Hz light flicker stimulates expression of diverse cytokines
560 with both immunomodulatory and neuro-protective properties.

561 It is important to note that our results were based on experiments done with male
562 mice. We chose to focus on males because we wanted to assess how 40Hz flicker,
563 which induces gamma oscillations, impacts neuroimmune signaling, building on
564 previous papers that have only studied this effect in male mice (Iaccarino et al., 2016;
565 Adaikkan et al., 2019; Martorell et al., 2019). However, we acknowledge that this is a
566 limitation of this study because there are effects of sex on immune response and
567 ovarian hormones have been shown to impact cytokine expression (Arakawa et al.,
568 2014; Cai et al., 2016). Future studies should further explore how this effect may differ
569 between the sexes.

570

571 **40Hz flicker cytokine response differs from acute inflammation**

572 We found that 40Hz flicker upregulates a profile of cytokines in a short period of
573 time, similar to an acute pro-inflammatory stimulus. However, previous work has shown
574 that 40Hz flicker has a neuro-protective effect. Therefore, we wanted to compare how
575 40Hz flicker induced cytokine expression differs from a known pro-inflammatory
576 stimulus operating under a similar acute time period.

577 Our analysis showed that 40Hz flicker stimulates expression of diverse cytokines
578 that differs from a model of acute inflammation. This difference was established by

579 comparing the LV1 cytokine profile of gamma sensory stimulation and acute LPS
580 inflammation. While there may be an overlap in some cytokines that were elevated, the
581 overall profiles are distinct between these two stimulations due to the differences in
582 magnitude of responses and the overall cytokines included. Two cytokines, GM-CSF,
583 and IL-2, significantly differed between 40Hz flicker and random stimulation but did not
584 differ between LPS and vehicle administration. The specific response of these two
585 cytokines to 40Hz flicker is especially interesting because GM-CSF may be both
586 neuroprotective and proinflammatory and low-dose IL-2 rescues cognitive and synaptic
587 plasticity deficits in a mouse model of AD (Bhattacharya et al., 2015; Alves et al., 2017;
588 Kiyota et al., 2018). Furthermore, the combination of GM-CSF and IL-2 has been
589 suggested to have synergistic effects. The combination of these cytokines has been
590 used to prevent immune dysregulation in multiple models of disease (Baiocchi et al.,
591 2001; Stagg et al., 2004; Elias et al., 2005). Thus the combination of these two
592 cytokines following 40Hz flicker may be neuroprotective.

593 Some cytokines significantly differed between both 40Hz versus random flicker
594 and LPS versus vehicle administration. An interesting observation from our data is that
595 while there was overlap in some of these cytokines, there was a noticeable difference in
596 the scale of separation between LPS and vehicle versus 40Hz and random stimulation.
597 While both were significantly upregulated by stimulation, LPS had a much larger effect
598 when compared to control condition. The magnitude of the cytokine response has been
599 suggested to alter a cytokine's effects (Saadoun et al., 2011; Shachar and Karin, 2013).
600 Thus, this low-dose increase caused by 40Hz flicker may be more responsible for the
601 neuroprotective effect of 40Hz flicker.

602 Lastly, IL-12p70, the bioactive form of the p35 and p40 combined IL-12 subunits,
603 was up-regulated in both LPS and 40Hz versus controls. In contrast, IP-10, which is
604 downstream of IL-12, was significantly different between LPS and control but not 40Hz
605 and random. IP-10 is induced by IFN- γ , which is a pro-inflammatory cytokine
606 downstream of IL-12 (Sgadari et al., 1996). This finding suggests that while both LPS
607 and 40Hz flicker may upregulate some similar cytokines, they may be leading to
608 different downstream mechanisms which explain why LPS is known to be neuro-toxic,
609 while 40Hz flicker is known to be neuroprotective (Iaccarino et al., 2016; Martorell et al.,
610 2019).

611

612 **40Hz flicker induces neuroimmune intracellular signal transduction pathways**

613 Our data show that 40Hz flicker stimulates NF κ B and MAPK pathway signaling,
614 which increased following 15 minutes or 60 minutes of 40Hz flicker, respectively,
615 followed by expression of cytokines. These findings are consistent with the known
616 transient kinetics of phospho-signaling and downstream gene and protein expression
617 (Janes et al., 2005; Gierut et al., 2015). While the effect of 5 minutes of 40Hz flicker on
618 the NF κ B pathway were not significant, many of the animals did separate on LV1 and
619 this was mostly driven by increases in TNFR1 and FADD phosphorylation. Interestingly,
620 these two proteins are upstream in the NF κ B pathway and therefore we would expect
621 these to become phosphorylated earlier than other proteins in the pathway. After 15
622 minutes of 40Hz flicker, all proteins in the NF κ B pathway had elevated phosphorylation
623 levels. Thus, we conclude that phosphorylation of the NF κ B pathway may begin after
624 around 5 minutes of 40Hz flicker in some animals, but the full effects may not be

625 detectable until after 15 minutes of 40Hz flicker. A similar trend is observed for the
626 MAPK pathway, but it seems to be later, where 15 minutes of 40Hz flicker begins to
627 upregulate the pathway and 60 minutes shows a distinct separation between 40Hz
628 flicker and random groups. Later onset of MAPK pathway activation may be related to
629 increased expression of cytokines that act through the MAPK pathway.

630 For phospho-protein analysis, we specifically compared 40Hz flicker and random
631 flicker exposure. We chose random flicker as our control because this stimulation type
632 controls for the largest number of stimulation variables. However, we anticipate that if
633 we compared 40Hz to 20Hz stimulation instead, we would see a bigger difference
634 between groups, since 20Hz had a more reduced cytokine expression profile in Figure 1.
635 In contrast, we anticipate that light stimulation may also upregulate signaling pathways.
636 We expect that because light stimulation uniquely upregulates some cytokines, distinct
637 from 40Hz flicker, that light may also upregulate some of the signaling pathways that
638 are known to regulate cytokines.

639 Interestingly, our data show that the NF κ B pathway is downregulated below
640 random flicker after 1hour of 40Hz flicker stimulation, suggesting the effects of 40Hz
641 flicker on these pathways are transient. Both NF κ B and MAPK pathways are highly
642 regulated via feedback mechanisms (Hutti et al., 2007; Lake et al., 2016). Given that our
643 observed changes are occurring over the course of an hour, negative feedback
644 mechanisms within the pathways are likely responsible for the downregulation of these
645 pathways.

646 Our hypothesized time-course of pathway activity is further supported when
647 examining correlations between phospho-proteins. After 5 minutes of 40Hz flicker, a

648 pattern emerged within each pathway. Specifically, in the NF κ B pathway, both pFADD
649 and TNFR1 were highly correlated with phosphorylation of each other protein, aligning
650 with increased expression patterns of these two phospho-proteins at the same time
651 course. TNFR1 is upstream in the NF κ B signaling pathway, suggesting 5 minutes of
652 flicker begins to modulate the top of the pathway. 15 minutes of 40Hz flicker revealed
653 more correlations among proteins, and these correlations included more proteins
654 downstream in the pathway, suggesting the pathway is progressively activated with
655 longer flicker exposure. However, after 60 minutes of 40Hz flicker, many correlations
656 were no longer present. In fact, in the MAPK pathway, only pATF-2 and pJnk were
657 correlated, downstream in the pathway. These correlation results help support our
658 activation data. However, we note that the small sample size (6 animals), might account
659 for the low significance associated with 60 minutes of stimulation at 40Hz. Further, while
660 the analysis was designed to reveal correlations between any phospho-proteins, all
661 significant correlations remained within each pathway, supporting the idea that each
662 pathway is operating with independent dynamics.

663 Both the NF κ B and MAPK pathways play key roles in immune function, synaptic
664 plasticity, and learning and memory. NF κ B and MAPK pathways regulate cytokine
665 levels by activating transcription factors involved in cytokine expression (Hommes et al.,
666 2003; Cloutier et al., 2007; Liu et al., 2017). Increased phosphorylation in the MAPK
667 pathway occurs after spatial memory and is necessary for long-term memory formation
668 (Blum et al., 1999). The NF κ B pathway is more traditionally known for its role in
669 inflammation, but is also necessary for long-term potentiation and long-term depression
670 and is increased following synaptic stimulation (C. and P., 1999; Meffert et al., 2003).

671 40Hz light flicker likely stimulates intracellular phospho-signaling and expression
672 of diverse genes by driving neural activity. Several studies have shown that flickering
673 light at a particular frequency drives that frequency neural activity in primary visual
674 areas and 40Hz flicker induces neural activity around 40Hz (Gray et al., 1989; Iaccarino
675 et al., 2016; Singer et al., 2018). Neuronal activity can lead to calcium influx which in
676 turn, stimulates multiple molecular signaling events, including activation of multiple
677 isoforms of protein kinase C (PKC), which can activate the NF κ B and MAPK pathways.
678 In fact, inhibition of calcium activity blocks NF κ B activation (Meffert et al., 2003). These
679 pathways provide a possible link between gamma frequency activity induced by 40Hz
680 flicker, phospho-signaling, and downstream gene expression.

681

682 **Behavior is similar across different visual stimulation conditions**

683 Cytokine expression can be modified by an animal's behavioral state, for
684 example when an animal is under stress (Minami et al., 1991; Ishikawa et al., 2001).
685 While it is known that chronic 40Hz flicker does not affect anxiolytic behaviors over time,
686 we wanted to ensure 40Hz flicker stimulation did not differentially affect animal behavior
687 in real time over the timescales of our analyses when compared to other stimulation
688 types (Martorell et al., 2019a). We measured total time spent in the center versus
689 surround areas of the enclosure and time spent active versus freezing. We concluded
690 that flicker stimulation did not invoke anxiety-like behavior or changes in overall activity
691 levels. To assess if one stimulation type was more aversive than others, we analyzed
692 time spent in the front of the cage where the lights were positioned versus the back and
693 found no differences across stimulation conditions. Interestingly, animals across all

694 conditions spent somewhat more time (~65%) in the back of the cage, which is not
695 surprising considering that mice tend to stay in dark areas if given the choice (Crawley
696 and Goodwin, 1980). Last, we measured the distance animals traveled within each
697 stimulation type and found no differences across flicker conditions. In short, our analysis
698 revealed no differences in any of our measured animal behaviors between stimulation
699 conditions. Therefore, our observations show that induced phospho-signaling and
700 cytokine expression after 40Hz light flicker cannot be explained by changes in animal
701 behavior.

702 In total, our results show that 40Hz flicker drives rapid signaling within the NF κ B
703 and is followed by activation of MAPK pathway and an upregulation of cytokines. The
704 diverse functions regulated by these pathways together with the diversity of cytokine
705 and growth factors expressed in response to 40Hz stimulation suggests that minutes of
706 flicker stimulation may induce changes in various cell and tissue functions that include
707 immune activity and neuronal and synaptic health. Furthermore, different forms of visual
708 stimulation induced unique cytokine profiles. Thus, flicker stimulation may be used to
709 rapidly and non-invasively manipulate signaling and expression of genes that go beyond
710 neural immune activity. Importantly, all our signaling analyses were conducted in wild-
711 type animals, helping establish the effects of 40Hz flicker stimulation independent of
712 disease pathology. Our work provides a foundation for flicker's therapeutic potential to
713 other disorders involving the neuroimmune system.

REFERENCES

- 714 Adaikkan C, Middleton SJ, Marco A, Pao P-C, Mathys H, Kim DN-W, Gao F, Young JZ,
715 Suk H-J, Boyden ES, McHugh TJ, Tsai L-H (2019) Gamma Entrainment Binds
716 Higher-Order Brain Regions and Offers Neuroprotection. *Neuron* Available at:
717 <https://www.sciencedirect.com/science/article/pii/S0896627319303460>.
- 718 Alves S, Churlaud G, Audrain M, Michaelsen-Preusse K, Fol R, Souchet B, Braudeau J,
719 Korte M, Klatzmann D, Cartier N (2017) Interleukin-2 improves amyloid pathology,
720 synaptic failure and memory in Alzheimer's disease mice. *Brain*.
- 721 Arakawa K, Arakawa H, Hueston CM, Deak T (2014) Effects of the estrous cycle and
722 ovarian hormones on central expression of interleukin-1 evoked by stress in female
723 rats. *Neuroendocrinology*.
- 724 Baier PC, May U, Scheller J, Rose-John S, Schifflholz T (2009) Impaired
725 hippocampus-dependent and -independent learning in IL-6 deficient mice. *Behav*
726 *Brain Res* 200:192–196 Available at:
727 <http://www.ncbi.nlm.nih.gov/pubmed/19378383>.
- 728 Baiocchi RA, Ward JS, Carrodegua L, Eisenbeis CF, Peng R, Roychowdhury S,
729 Vourganti S, Sekula T, O'Brien M, Moeschberger M, Caligiuri MA (2001) GM-CSF
730 and IL-2 induce specific cellular immunity and provide protection against Epstein-
731 Barr virus lymphoproliferative disorder. *J Clin Invest*.
- 732 Barroeta-Espar I et al. (2019) Distinct cytokine profiles in human brains resilient to
733 Alzheimer's pathology. *Neurobiol Dis* 121:327–337 Available at:
734 <https://www.sciencedirect.com/science/article/pii/S0969996118307137>.

- 735 Bhattacharya P, Budnick I, Singh M, Thiruppathi M, Alharshawi K, Elshabrawy H,
736 Holterman MJ, Prabhakar BS (2015) Dual Role of GM-CSF as a Pro-Inflammatory
737 and a Regulatory Cytokine: Implications for Immune Therapy. *J Interf Cytokine Res.*
738 Blum S, Moore AN, Adams F, Dash PK (1999) A Mitogen-Activated Protein Kinase
739 Cascade in the CA1/CA2 Subfield of the Dorsal Hippocampus Is Essential for
740 Long-Term Spatial Memory. Available at:
741 <http://www.jneurosci.org/content/jneuro/19/9/3535.full.pdf>.
- 742 Bowen KK, Dempsey RJ, Vemuganti R (2011) Adult interleukin-6 knockout mice show
743 compromised neurogenesis. *Neuroreport* 22:126–130 Available at:
744 <http://www.ncbi.nlm.nih.gov/pubmed/21266900>.
- 745 C. AB, P. MM (1999) Evidence for the involvement of TNF and NF- κ B in hippocampal
746 synaptic plasticity. *Synapse* 35:151–159.
- 747 Cai KC, van Mil S, Murray E, Mallet JF, Matar C, Ismail N (2016) Age and sex
748 differences in immune response following LPS treatment in mice. *Brain Behav*
749 *Immun.*
- 750 Calsolaro V, Edison P (2016) Neuroinflammation in Alzheimer's disease: Current
751 evidence and future directions. *Alzheimers Dement* 12:719–732 Available at:
752 <http://www.ncbi.nlm.nih.gov/pubmed/27179961>.
- 753 Chen T, Wu Y, Wang Y, Zhu J, Chu H, Kong L, Yin L, Ma H (2017) Brain-Derived
754 Neurotrophic Factor Increases Synaptic Protein Levels via the MAPK/Erk Signaling
755 Pathway and Nrf2/Trx Axis Following the Transplantation of Neural Stem Cells in a
756 Rat Model of Traumatic Brain Injury. *Neurochem Res* 42:3073–3083 Available at:
757 <http://link.springer.com/10.1007/s11064-017-2340-7>.

- 758 Cloutier A, Ear T, Blais-Charron E, Dubois CM, McDonald PP (2007) Differential
759 involvement of NF- κ B and MAP kinase pathways in the generation of inflammatory
760 cytokines by human neutrophils. *J Leukoc Biol* 81:567–577 Available at:
761 <http://www.ncbi.nlm.nih.gov/pubmed/17062602>.
- 762 Crawley JN, Goodwin FK (1980) Preliminary report of a simple animal model for the
763 behavioral actions of benzodiazepines. *Pharmacol Biochem Behav* 13:167–170.
- 764 De Filippo K, Dudeck A, Hasenberg M, Nye E, Van Rooijen N, Hartmann K, Gunzer M,
765 Roers A, Hogg N (2013) Mast cell and macrophage chemokines CXCL1/CXCL2
766 control the early stage of neutrophil recruitment during tissue inflammation. *Blood*
767 121:4930–4937 Available at:
768 [http://www.bloodjournal.org.proxy.library.emory.edu/content/121/24/4930.long?ssoc-
769 checked=true](http://www.bloodjournal.org.proxy.library.emory.edu/content/121/24/4930.long?ssoc-checked=true).
- 770 Decourt B, Lahiri DK, Sabbagh MN (2017) Targeting Tumor Necrosis Factor Alpha for
771 Alzheimer's Disease. *Curr Alzheimer Res* 14:412–425 Available at:
772 <http://www.ncbi.nlm.nih.gov/pubmed/27697064>.
- 773 Donegan JJ, Girotti M, Weinberg MS, Morilak DA (2014) A novel role for brain
774 interleukin-6: facilitation of cognitive flexibility in rat orbitofrontal cortex. *J Neurosci*
775 34:953–962 Available at: <http://www.ncbi.nlm.nih.gov/pubmed/24431453>.
- 776 Eisen MB, Spellman PT, Brown PO, Botstein D (1998) Cluster analysis and display of
777 genome-wide expression patterns. *Proc Natl Acad Sci U S A* 95:14863–14868
778 Available at: <http://www.ncbi.nlm.nih.gov/pubmed/9843981>.
- 779 Elias EG, Zapas JL, Beam SL, Brown SD (2005) GM-CSF and IL-2 combination as
780 adjuvant therapy in cutaneous melanoma: early results of a phase II clinical trial.

- 781 Oncology (Williston Park).
- 782 Elmore MRP, Najafi AR, Koike MA, Dagher NN, Spangenberg EE, Rice RA, Kitazawa M,
783 Matusow B, Nguyen H, West BL, Green KN (2014) Colony-stimulating factor 1
784 receptor signaling is necessary for microglia viability, unmasking a microglia
785 progenitor cell in the adult brain. *Neuron* 82:380–397 Available at:
786 <http://www.ncbi.nlm.nih.gov/pubmed/24742461>.
- 787 Eriksson, L.; Byrne, T.; Johansson, E.; Trygg, J.; Vikström C (2006) Multi- and
788 Megavariate Data Analysis. Basic principles and applications.
- 789 Fenn AM, Hall JCE, Gensel JC, Popovich PG, Godbout JP (2014) IL-4 signaling drives
790 a unique arginase+/IL-1 β + microglia phenotype and recruits macrophages to the
791 inflammatory CNS: consequences of age-related deficits in IL-4R α after traumatic
792 spinal cord injury. *J Neurosci* 34:8904–8917 Available at:
793 <http://www.ncbi.nlm.nih.gov/pubmed/24966389>.
- 794 Gabellec MM, Griffais R, Fillion G, Haour F (1995) Expression of interleukin 1 α ,
795 interleukin 1 β and interleukin 1 receptor antagonist mRNA in mouse brain:
796 regulation by bacterial lipopolysaccharide (LPS) treatment. *Mol Brain Res*.
- 797 Ghersa P, Gelati M, Colinge J, Feger G, Power C, Ghersa P, Gelati M, Colinge J, Feger
798 G, Power C, Papoian R, Salmaggi A (2002) MIG--differential gene expression in
799 mouse brain endothelial cells. *Neuroreport* 13:9–14 Available at:
800 <http://www.ncbi.nlm.nih.gov/pubmed/11924901>.
- 801 Gierut JJ, Wood LB, Lau KS, Lin Y-J, Genetti C, Samatar AA, Lauffenburger DA, Haigis
802 KM (2015) Network-level effects of kinase inhibitors modulate TNF- α -induced
803 apoptosis in the intestinal epithelium. *Sci Signal* 8:ra129 Available at:

- 804 <http://www.ncbi.nlm.nih.gov/pubmed/26671150>.
- 805 Golland P, Liang F, Mukherjee S, Panchenko D (2010) Permutation Tests for
806 Classification.
- 807 Goshen I, Kreisel T, Ounallah-Saad H, Renbaum P, Zalstein Y, Ben-Hur T, Levy-
808 Lahad E, Yirmiya R (2007) A dual role for interleukin-1 in hippocampal-dependent
809 memory processes. *Psychoneuroendocrinology* 32:1106–1115 Available at:
810 <https://linkinghub.elsevier.com/retrieve/pii/S0306453007002120>.
- 811 Gray CM, König P, Engel AK, Singer W (1989) Oscillatory responses in cat visual cortex
812 exhibit inter-columnar synchronization which reflects global stimulus properties.
813 *Nature* 338:334–337 Available at: <http://www.ncbi.nlm.nih.gov/pubmed/2922061>.
- 814 Hanisch U-K (2002) Microglia as a source and target of cytokines. *Glia* 40:140–155
815 Available at: <http://www.ncbi.nlm.nih.gov/pubmed/12379902>.
- 816 Hommes DW, Peppelenbosch MP, van Deventer SJH (2003) Mitogen activated protein
817 (MAP) kinase signal transduction pathways and novel anti-inflammatory targets.
818 *Gut* 52:144–151 Available at: <http://www.ncbi.nlm.nih.gov/pubmed/12477778>.
- 819 Hutti JE, Turk BE, Asara JM, Ma A, Cantley LC, Abbott DW (2007) I B Kinase
820 Phosphorylates the K63 Deubiquitinase A20 To Cause Feedback Inhibition of the
821 NF- B Pathway. *Mol Cell Biol* 27:7451–7461 Available at:
822 <https://mcb.asm.org/content/27/21/7451.short>.
- 823 Iaccarino HF, Singer AC, Martorell AJ, Rudenko A, Gao F, Gillingham TZ, Mathys H,
824 Seo J, Kritskiy O, Abdurrob F, Adaikkan C, Canter RG, Rueda R, Brown EN,
825 Boyden ES, Tsai L-H (2016) Gamma frequency entrainment attenuates amyloid

- 826 load and modifies microglia. *Nature* 540:230–235 Available at:
827 <http://www.nature.com/doi/10.1038/nature20587> [Accessed April 26, 2019].
- 828 Imai Y, Kohsaka S (2002) Intracellular signaling in M-CSF-induced microglia activation:
829 role of Iba1. *Glia* 40:164–174 Available at:
830 <http://www.ncbi.nlm.nih.gov/pubmed/12379904>.
- 831 Ishikawa I, Kitamura H, Kimura K, Saito M (2001) Brain interleukin-1 is involved in blood
832 interleukin-6 response to immobilization stress in rats. *Jpn J Vet Res* 49:19–25
833 Available at:
834 [https://pdfs.semanticscholar.org/8bb2/c97825f035ce2736ee52717042a3494b40dd](https://pdfs.semanticscholar.org/8bb2/c97825f035ce2736ee52717042a3494b40dd.pdf).
835 pdf.
- 836 Janes KA, Albeck JG, Gaudet S, Sorger PK, Lauffenburger DA, Yaffe MB (2005) Cell
837 signaling: A systems model of signaling identifies a molecular basis set for
838 cytokine-induced apoptosis. *Science* (80-) 310:1646–1653.
- 839 Johnson EA, Dao TL, Guignet MA, Geddes CE, Koemeter-Cox AI, Kan RK (2011)
840 Increased expression of the chemokines CXCL1 and MIP-1 α by resident brain cells
841 precedes neutrophil infiltration in the brain following prolonged soman-induced
842 status epilepticus in rats. *J Neuroinflammation* 8:41 Available at:
843 <http://jneuroinflammation.biomedcentral.com/articles/10.1186/1742-2094-8-41>.
- 844 Kaltschmidt B, Ndiaye D, Korte M, Pothion S, Arbibe L, Prüllage M, Pfeiffer J, Lindecke
845 A, Staiger V, Israël A, Kaltschmidt C, Mémet S (2006) NF-kappaB regulates spatial
846 memory formation and synaptic plasticity through protein kinase A/CREB signaling.
847 *Mol Cell Biol* 26:2936–2946.
- 848 Kanonidis EI, Roy MM, Deighton RF, Le Bihan T (2016) Protein Co-Expression Analysis

- 849 as a Strategy to Complement a Standard Quantitative Proteomics Approach: Case
850 of a Glioblastoma Multiforme Study. *PLoS One* 11:e0161828 Available at:
851 <http://www.ncbi.nlm.nih.gov/pubmed/27571357>.
- 852 Kiyota T, Machhi J, Lu Y, Dyavarshetty B, Nemati M, Yokoyama I, Lee Mosley R,
853 Gendelman HE (2018) Granulocyte-macrophage colony-stimulating factor
854 neuroprotective activities in Alzheimer's disease mice. *J Neuroimmunol*.
- 855 Lake D, Corrêa SAL, Müller J (2016) Negative feedback regulation of the ERK1/2
856 MAPK pathway. *Cell Mol Life Sci* 73:4397–4413 Available at:
857 <http://www.ncbi.nlm.nih.gov/pubmed/27342992>.
- 858 Latta CH, Sudduth TL, Weekman EM, Brothers HM, Abner EL, Popa GJ, Mendenhall
859 MD, Gonzalez-Oregon F, Braun K, Wilcock DM (2015) Determining the role of IL-4
860 induced neuroinflammation in microglial activity and amyloid- β using BV2 microglial
861 cells and APP/PS1 transgenic mice. *J Neuroinflammation* 12:41.
- 862 Lee YH, Kim SH, Kim Y, Lim Y, Ha K, Shin SY (2012) Inhibitory effect of the
863 antidepressant imipramine on NF- κ B-dependent CXCL1 expression in TNF α -
864 exposed astrocytes. *Int Immunopharmacol* 12:547–555 Available at:
865 <https://www.sciencedirect.com/science/article/pii/S1567576912000318?via%3Dihub>
866 b.
- 867 Liu T, Zhang L, Joo D, Sun S-C (2017) NF- κ B signaling in inflammation. *Signal*
868 *Transduct Target Ther* 2 Available at:
869 <http://www.ncbi.nlm.nih.gov/pubmed/29158945>.
- 870 Martorell AJ, Paulson AL, Suk H-J, Abdurrob F, Drummond GT, Guan W, Young JZ,
871 Kim DN-W, Kritskiy O, Barker SJ, Mangena V, Prince SM, Brown EN, Chung K,

- 872 Boyden ES, Singer AC, Tsai L-H (2019a) Multi-sensory Gamma Stimulation
873 Ameliorates Alzheimer's-Associated Pathology and Improves Cognition. *Cell*
874 177:256-271.e22 Available at: <http://www.ncbi.nlm.nih.gov/pubmed/30879788>.
- 875 Martorell AJ, Paulson AL, Suk HJ, Abdurrob F, Drummond GT, Guan W, Young JZ, Kim
876 DNW, Kritskiy O, Barker SJ, Mangena V, Prince SM, Brown EN, Chung K, Boyden
877 ES, Singer AC, Tsai LH (2019b) Multi-sensory Gamma Stimulation Ameliorates
878 Alzheimer's-Associated Pathology and Improves Cognition. *Cell* 177:256-271.e22.
- 879 Mattson MP, Meffert MK (2006) Roles for NF- κ B in nerve cell survival, plasticity, and
880 disease. *Cell Death Differ* 13:852–860 Available at:
881 <http://www.nature.com/articles/4401837>.
- 882 Meffert MK, Chang JM, Wiltgen BJ, Fanselow MS, Baltimore D (2003) NF- κ B functions
883 in synaptic signaling and behavior. *Nat Neurosci* 6:1072–1078 Available at:
884 <http://www.nature.com/articles/nn1110>.
- 885 Meneses G, Rosetti M, Espinosa A, Florentino A, Bautista M, Díaz G, Olvera G,
886 Bárcena B, Fleury A, Adalid-Peralta L, Lamoyi E, Fragoso G, Sciotto E (2018)
887 Recovery from an acute systemic and central LPS-inflammation challenge is
888 affected by mouse sex and genetic background. *PLoS One*.
- 889 Minami M, Kuraishi Y, Yamaguchi T, Nakai S, Hirai Y, Satoh M (1991) Immobilization
890 stress induces interleukin-1 β mRNA in the rat hypothalamus. *Neurosci Lett*
891 123:254–256 Available at:
892 <https://www.sciencedirect.com/science/article/abs/pii/0304394091909440>.
- 893 Mitrasinovic OM, Murphy GM (2003) Microglial overexpression of the M-CSF receptor
894 augments phagocytosis of opsonized Abeta. *Neurobiol Aging* 24:807–815 Available

- 895 at: <http://www.ncbi.nlm.nih.gov/pubmed/12927763>.
- 896 Neniskyte U, Vilalta A, Brown GC (2014) Tumour necrosis factor alpha-induced
897 neuronal loss is mediated by microglial phagocytosis. *FEBS Lett* 588:2952–2956
898 Available at: <http://www.ncbi.nlm.nih.gov/pubmed/24911209>.
- 899 Prieto GA, Cotman CW (2017) Cytokines and cytokine networks target neurons to
900 modulate long-term potentiation. *Cytokine Growth Factor Rev* 34:27–33 Available
901 at: <http://www.ncbi.nlm.nih.gov/pubmed/28377062>.
- 902 Qin L, Wu X, Block ML, Liu Y, Breese GR, Hong JS, Knapp DJ, Crews FT (2007)
903 Systemic LPS causes chronic neuroinflammation and progressive
904 neurodegeneration. *Glia*.
- 905 Rappert A (2004) CXCR3-Dependent Microglial Recruitment Is Essential for Dendrite
906 Loss after Brain Lesion. *J Neurosci* 24:8500–8509 Available at:
907 <http://www.ncbi.nlm.nih.gov/pubmed/15456824>.
- 908 Ringheim GE, Szczepanik AM, Petko W, Burgher KL, Zhu SZ, Chao CC (1998)
909 Enhancement of beta-amyloid precursor protein transcription and expression by the
910 soluble interleukin-6 receptor/interleukin-6 complex. *Brain Res Mol Brain Res*
911 55:35–44 Available at: <http://www.ncbi.nlm.nih.gov/pubmed/9645958>.
- 912 Saadoun D, Rosenzweig M, Joly F, Six A, Carrat F, Thibault V, Sene D, Cacoub P,
913 Klatzmann D (2011) Regulatory T-cell responses to low-dose interleukin-2 in HCV-
914 induced vasculitis. *N Engl J Med*.
- 915 Sgadari C, Angiolillo AL, Tosato G (1996) Inhibition of angiogenesis by interleukin-12 is
916 mediated by the interferon-inducible protein 10. *Blood*.

- 917 Shachar I, Karin N (2013) The dual roles of inflammatory cytokines and chemokines in
918 the regulation of autoimmune diseases and their clinical implications. *J Leukoc Biol.*
- 919 Sheridan GK, Murphy KJ (2013) Neuron-glia crosstalk in health and disease:
920 Fractalkine and CX3CR1 take centre stage. *Open Biol* 3:130181 Available at:
921 <http://rsob.royalsocietypublishing.org/cgi/doi/10.1098/rsob.130181>.
- 922 Singer AC, Martorell AJ, Douglas JM, Abdurrob F, Attokaren MK, Tipton J, Mathys H,
923 Adaikkan C, Tsai LH (2018) Noninvasive 40-Hz light flicker to recruit microglia and
924 reduce amyloid beta load. *Nat Protoc* 13:1850–1868.
- 925 Stagg J, Wu JH, Bouganim N, Galipeau J (2004) Granulocyte-macrophage colony-
926 stimulating factor and interleukin-2 fusion cDNA for cancer gene immunotherapy.
927 *Cancer Res.*
- 928 Stellwagen D, Malenka RC (2006) Synaptic scaling mediated by glial TNF- α . *Nature*
929 440:1054–1059 Available at: <http://www.ncbi.nlm.nih.gov/pubmed/16547515>.
- 930 Sweatt JD (2001) The neuronal MAP kinase cascade: a biochemical signal integration
931 system subserving synaptic plasticity and memory. *J Neurochem* 76:1–10 Available
932 at: <http://www.ncbi.nlm.nih.gov/pubmed/11145972>.
- 933 Ure DR, Lane TE, Liu MT, Rodriguez M (2005) Neutralization of chemokines RANTES
934 and MIG increases virus antigen expression and spinal cord pathology during
935 Theiler's virus infection. *Int Immunol* 17:569–579.
- 936 Wang GY, Taylor T, Sumich A, Merien F, Borotkanics R, Wrapson W, Krägeloh C,
937 Siegert RJ (2017) Associations between immunological function and memory recall
938 in healthy adults. *Brain Cogn* 119:39–44 Available at:

939 <http://www.ncbi.nlm.nih.gov/pubmed/29020639>.

940 Wohleb ES, Franklin T, Iwata M, Duman RS (2016) Integrating neuroimmune systems

941 in the neurobiology of depression. *Nat Rev Neurosci* 17:497–511 Available at:

942 <http://www.ncbi.nlm.nih.gov/pubmed/27277867>.

943

FIGURE LEGENDS

Figure 1: One hour of 40Hz flicker increased cytokine expression in visual cortex

- A) Experimental configuration for presenting visual stimulation.
- B) Cytokine expression in visual cortices of mice exposed to 1 hour of visual stimulation. Each row represents one animal (n=6). Cytokines (columns) are arranged in order of their weights on the first latent variable (LV1) in (D). Color indicates z-scored expression levels for each cytokine. Top four cytokines from LV1 are boxed in red.
- C) Partial least squares discriminant analysis (PLSDA) identified LV1, the axis which separated 40Hz flicker exposed animals (red) to the right, 20Hz flicker (blue) and constant light (green) exposed animals to the left and random (black) flicker exposed animals toward the middle (dots indicate individual animals for all graphs in this figure). LV2 separated 20Hz, random, and light conditions.
- D) The weighted profile of cytokines that make up LV1 based on which cytokines best correlated with separation of 40Hz (positive) versus flicker control groups (negative). (mean \pm SD from a leave one out cross validation).
- E) LV1 scores were significantly different for 40Hz group compared to controls (mean \pm SEM; $F(3, 20) = 5.855$, $p = 0.0049$, one-way ANOVA). Each dot represents one animal. Results were confirmed with shuffling analysis (see Methods).
- F) There were significant differences in expression of most of the top four analytes, M-CSF, IL-6, MIG, and IL-4 when assessed individually. P-values for comparisons between groups are listed in the figure. For one-way ANOVA comparisons across all groups: M-CSF: $F(3,20) = 2.970$, $p = 0.0564$, IL-6: $F(3,20) = 3.775$, $p = 0.0269$, MIG: $F(3,20) = 4.532$, $p = 0.0140$, and IL-4: $F(3,20) = 2.051$, $p = 0.1391$.

G) There were significant differences in expression of IFN- γ , IL-12p70, GM-CSF, IL-7, and IL-1 β as well. P-values for comparisons between groups are listed in the figure. For one-way ANOVA comparisons across all groups: IFN- γ : $F(3,20)=6.32$, $p=0.0034$), IL-12p70: $F(3,20)=6.428$, $p=0.0032$), GM-CSF: $F(3,20)=4.13$, $p=0.0197$), IL-7: $F(3,20)=9.541$, $p=0.0004$), and IL-1 β : $F(3,20)=3.404$, $p=0.0377$).

Figure 2: Flicker control conditions each lead to unique cytokine expression

- A) The weighted profile of cytokines that make up LV2 based on which cytokines best correlated with separation of random (positive) versus 20Hz versus light flicker control groups (negative). (Mean \pm SD from a leave one out cross validation).
- B) LV2 scores were significantly different for all 4 groups (mean \pm SEM; $F(3, 20) =21.77$, $p<0.0001$, one-way ANOVA). Each dot represents one animal. P-values from Tukey's multiple comparison test are listed.
- C) Diagram of cytokine expression, with each cytokine name arranged based on expression per group.
- D) One-way ANOVA displays significant difference in IL-10 expression across groups (mean \pm SEM; $F(3, 20) =27.29$, $p<0.0001$, one-way ANOVA). P-values from Tukey's multiple comparison test are listed.
- E) As in **D** for IL-15 expression across groups (mean \pm SEM; $F(3, 20) =11.33$, $p=0.0001$, one-way ANOVA).
- F) As in **D** for RANTES expression across groups (mean \pm SEM; $F(3, 20) =11.48$, $p=0.0001$, one-way ANOVA).

- G) As in **D** for IL-2 expression across groups (mean \pm SEM; $F(3, 20) = 9.366$, $p = 0.0005$, one-way ANOVA).
- H) As in **D** for VEGF expression across groups (mean \pm SEM; $F(3, 20) = 6.790$, $p = 0.0024$, one-way ANOVA).
- I) As in **D** for IL-9 expression across groups (mean \pm SEM; $F(3, 20) = 4.076$, $p = 0.0207$, one-way ANOVA).

Figure 3: NF κ B phospho-protein signaling in visual cortex increased in response to 15 minutes of 40Hz flicker

- A) Simplified diagram of NF κ B signaling including phospho-proteins quantified in the present study (blue ovals).
- B) NF κ B phospho-protein expression in visual cortex in mice exposed to 5 minutes of 40Hz or random flicker (z-scored). Each row represents one animal with groups separated by thicker black horizontal lines. 23 total animals were analyzed, $n = 17$ in 40Hz group, $n = 6$ in random group; outliers removed through a principle component analysis on the data and iterative removal of data points outside a 99.5% confidence ellipse (mahalanobisQC in R v 3.5.2).
- C) As in (B) for mice exposed to 15 minutes of 40Hz or random flicker. 40Hz $n = 12$, random $n = 6$.
- D) As in (B) for mice exposed to 60 minutes of 40Hz or random flicker. 40Hz $n = 6$, random $n = 6$.
- E) *Top*: PLSDA on phospho-signaling data for mice exposed to 5 minutes of flicker, separating 40Hz (red) exposed animal to the right and random (black) to the left,

- along LV1. *Bottom*: Plot of LV1 scores between groups show a trend toward higher LV1 scores in 40Hz exposed animals (difference between means \pm SEM = -0.1943 ± 0.09455 ; $t(21) = 2.065$, $p = 0.0525$, two-tailed t-test). Dots indicate individual animals for all graphs in this figure.
- F) *Top*: As in (E) for mice exposed to 15 minutes of 40Hz or random flicker. *Bottom*: Plot of LV1 scores between groups reveal significantly higher LV1 scores in 40Hz exposed animals (difference between means \pm SEM = -0.3721 ± 0.08351 ; $t(16) = 4.456$, $p = 0.0004$, two-tailed t-test). Results were confirmed with permutation analysis (see Methods).
- G) *Top*: As in (E) for mice exposed to 60 minutes of 40Hz or random flicker. *Bottom*: Plot of LV1 scores between groups show no significant difference (difference between means \pm SEM = -0.2829 ± 0.2 ; $t(8) = 1.415$, $p = 0.1948$, two-tailed t-test).
- H) The weighted profile of NF κ B phospho-proteins that make up LV1 based on which phospho-proteins best correlated with 40Hz (positive) or random (negative) after 5 minutes of flicker exposure (mean \pm SD from a leave one out cross validation). pIKK α/β and TNFR1 most strongly contributed to separation between the groups
- I) As in (H) for 15 minutes of flicker. pFADD expression in 40Hz flicker group and pNF κ B in random group most strongly contributed to separation between groups.
- J) As in (H) for 60 minutes of flicker.

Figure 4: MAPK phospho-protein signaling in visual cortex increased in response to 60 minutes of 40Hz flicker

- A) Simplified diagram of MAPK signaling diagram including phospho-proteins quantified in the present study (blue ovals).
- B) MAPK phospho-protein expression in visual cortex in mice exposed to 5 minutes of 40Hz or random flicker (z-scored). Each row represents one animal with groups separated by thicker black horizontal lines. 34 total animals were analyzed, n=24 in 40Hz group, n=10 in random group; outliers removed through a principle component analysis on the data and iterative removal of data points outside a 99.5% confidence ellipse (mahalanobisQC in R v 3.5.2).
- C) As in (B) for mice exposed to 15 minutes of 40Hz or random flicker. 40Hz n=8, random n=6.
- D) As in (B) for mice exposed to 60 minutes of 40Hz or random flicker.
- E) *Top*: PLSDA on phospho-signaling data for mice exposed to 5 minutes of flicker did not separate 40Hz (red) samples and random (black) along LV1. *Bottom*: Plot of LV1 scores per group show no significant differences between groups (difference between means \pm SEM = -0.1181 ± 0.06318 ; $t(32) = 1.870, p = 0.0707$, unpaired two-tailed t-test). Dots indicate individual animals for all graphs in this figure.
- F) *Top*: As in (E) for mice exposed to 15 minutes of 40Hz or random flicker. *Bottom*: Plot of LV1 scores per group reveal a non-significant increase in 40Hz LV1 expression in 40Hz exposed animals. (-0.1572 ± 0.1311 ; $t(8.582) = 1.199, p = 0.2624$, unpaired t test with Welch's correction).
- G) *Top*: As in (E) for mice exposed to 15 minutes of 40Hz or random flicker. *Bottom*: Plot of LV1 scores per group show significantly higher LV1 scores in 40Hz exposed animals (-0.4393 ± 0.1185 ; $t(10) = 3.709, p = 0.0040$, two-tailed t-test).

- H) The weighted profile of MAPK phospho-proteins that make up LV1 based on which best correlated with 40Hz (positive) or random (negative) flicker after 5 minutes of flicker exposure (mean \pm SD from a leave one out cross validation).
- I) As in (H) for 15 minutes of flicker.
- J) As in (H) for 60 minutes of flicker. pMSK and pMEK expression in 40Hz flicker group most strongly contributed to separation between groups.

Figure 5: Phosphoprotein network correlations are highest after 15 minutes of 40Hz flicker exposure

- A) Significant correlations following 5 minutes of 40Hz flicker in NF κ B (orange) and MAPK (green) phosphoprotein levels across animals displayed as links, with color indicating the strength of positive (red) or negative correlations (blue). No negative correlations were found in these interactions. $q < 0.1$, false discover rate correction for 135 comparisons, Pearson correlation test. *Right*: Example correlated phospho-proteins.
- B) As in (A) for 15 minutes of 40Hz flicker.
- C) As in (A) for 60 minutes of 40Hz flicker.

Figure 6: 40Hz flicker does not alter animal behavior during exposure

- A) Example heatmap representing the amount of time spent in locations within the flicker enclosure. Delineations indicating the center, front, and back of the cage were used for behavior analysis.

- B) Total percentage of time animals in each group spent in the center of the cage (F (3, 15) = 0.8754, p = 0.4757, RM-ANOVA). Error bars indicate mean \pm SEM. A total of 5 animals were used, represented by dots indicating individual animals for all bar graphs in this Figure (Red=40Hz, Black=random, Blue=20Hz, Green=light).
- C) Total percentage of time animals in each group spent active (versus freezing) (F (3, 15) = 0.9306, p = 0.4502, RM-ANOVA).
- D) Total percentage of time animals in each group spend in the back half of the cage (versus front) (F (3, 15) = 0.1727, p = 0.9132, RM-ANOVA).
- E) Total distance animals in each group traveled during stimulation (F (3, 15) = 0.3392, p = 0.7973, RM-ANOVA).

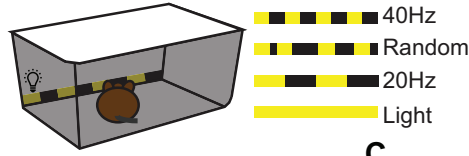
Figure 7: 40Hz flicker differs from LPS-induced acute inflammation.

- A) The weighted profile of cytokines that make up LV1 following 40Hz flicker (blue) or LPS (orange) (mean \pm SD from a leave one out cross validation).
- B) GM-CSF and IL-2 expression levels significantly differed in 40Hz versus random ("Flicker") but not LPS versus vehicle ("Acute Inflammation"). P-values for t-test comparisons between groups are listed in figure.
- C) IL-12p70, Eotaxin, TNF- α , and MCP1 expression levels significantly differed for both 40Hz versus random and LPS versus vehicle. P-values for t-test comparisons between groups are listed in figure.
- D) G-CSF, KC, RANTES, IP-10, IL-4, and MIC expression levels significantly differed for LPS versus vehicle but not 40Hz versus random. P-values for t-test comparisons between groups are listed in figure.

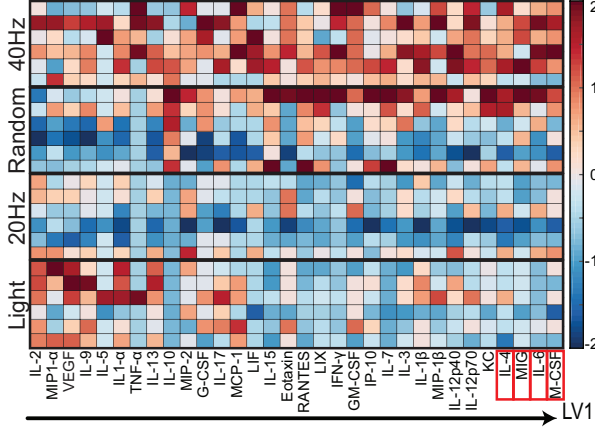
Video 1:

Example video of mouse undergoing flicker stimulation. Note, this video shows 20Hz flicker because 40Hz flicker is too fast to capture with standard movie frame rates.

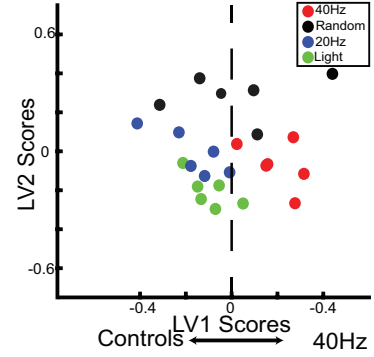
A Schematic of Sensory Stimulation



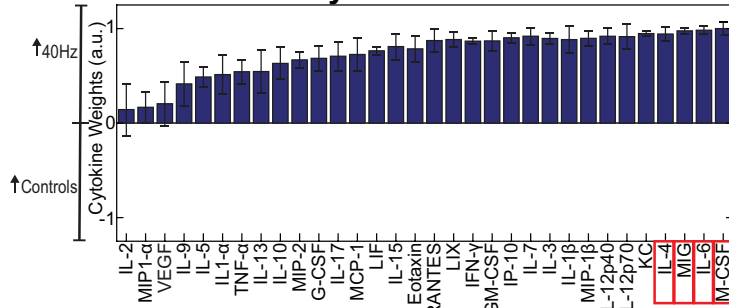
B Cytokine Expression Following Flicker



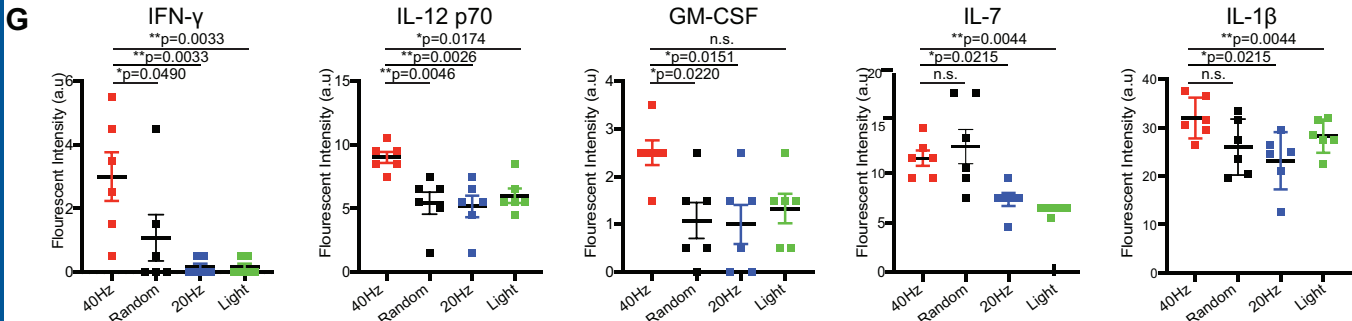
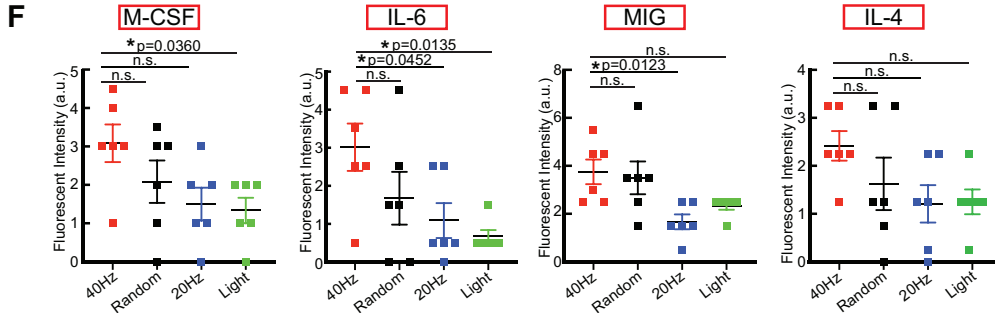
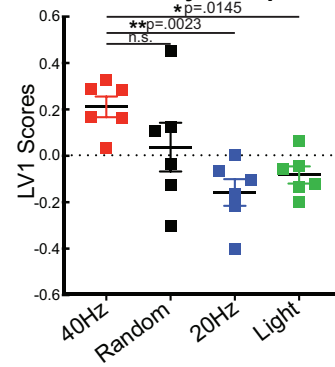
C PLSDA

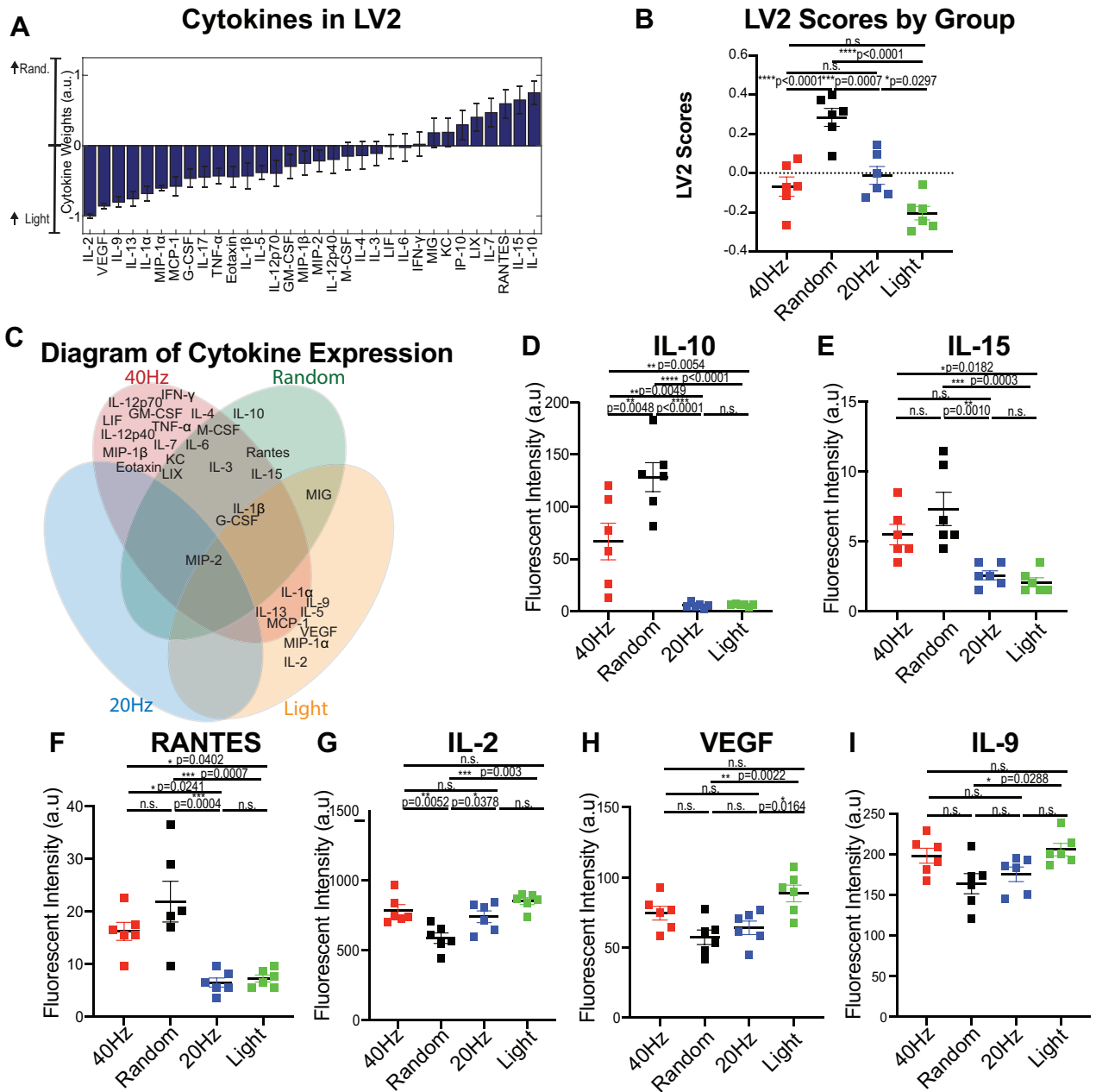


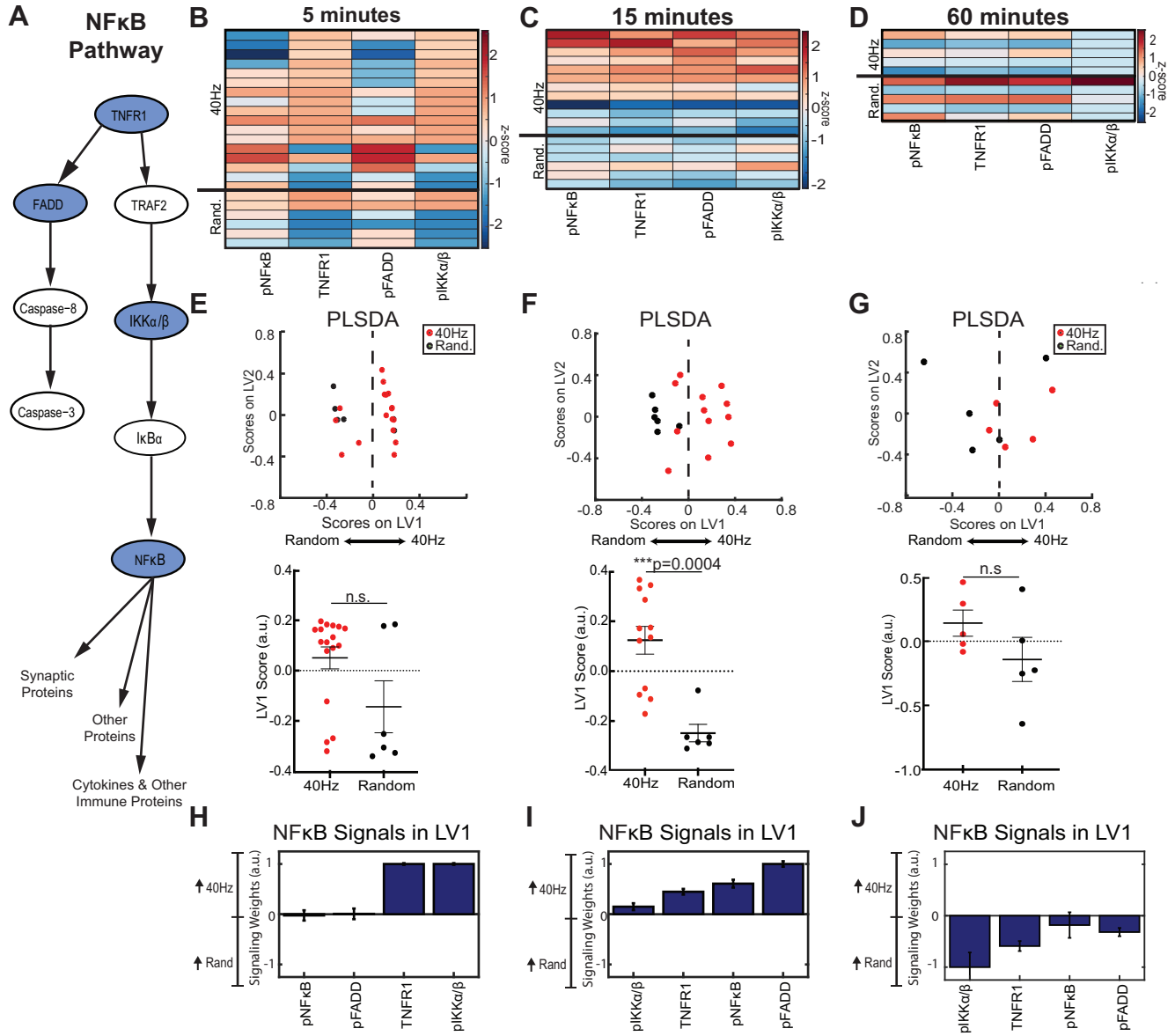
D Cytokines in LV1

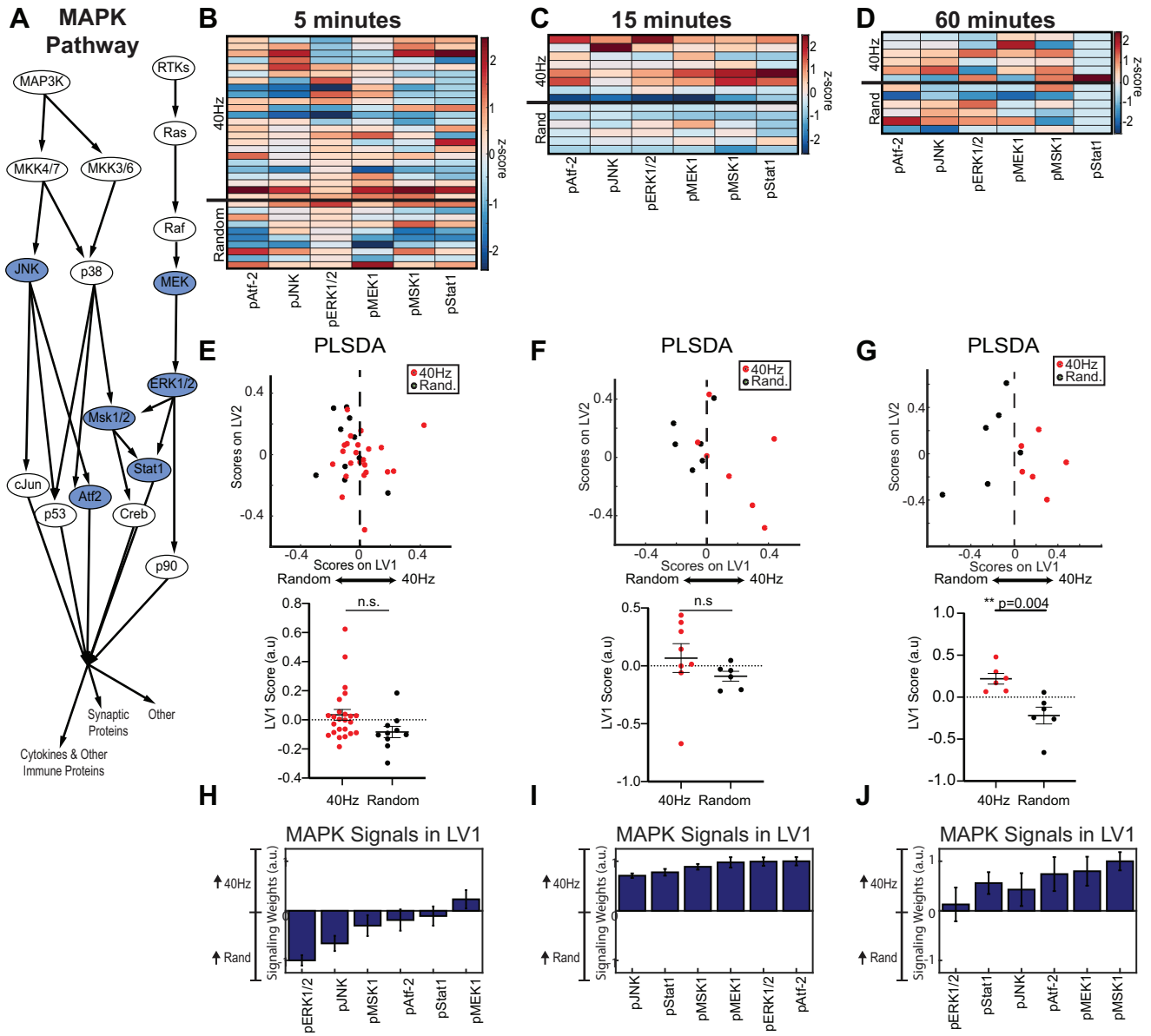


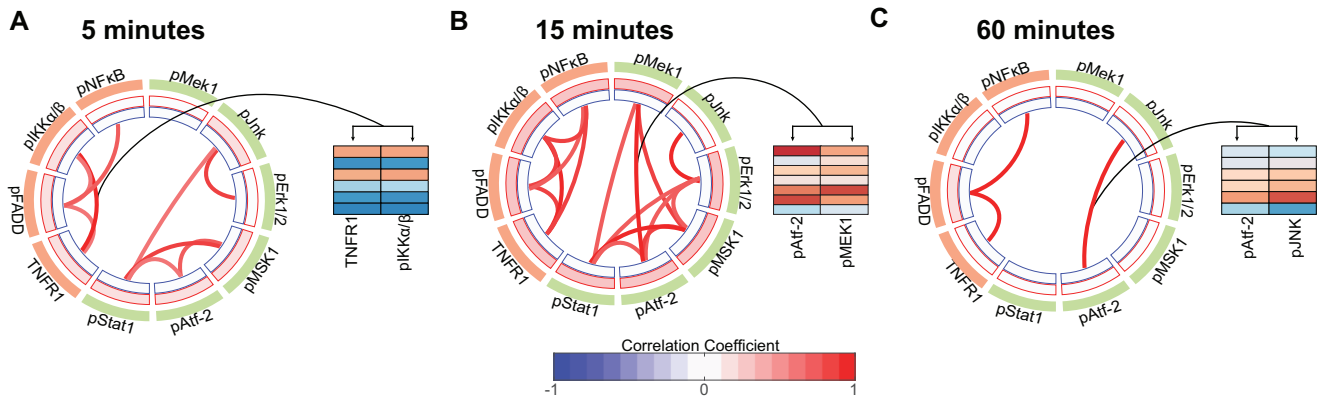
E LV1 Scores by Groups



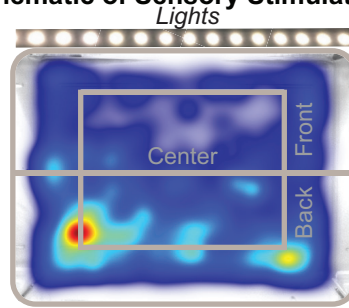




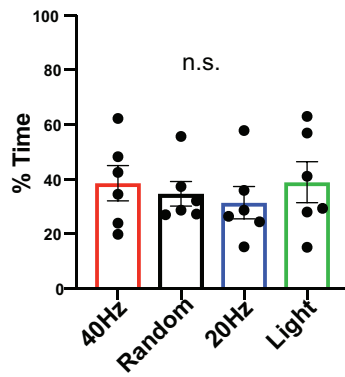




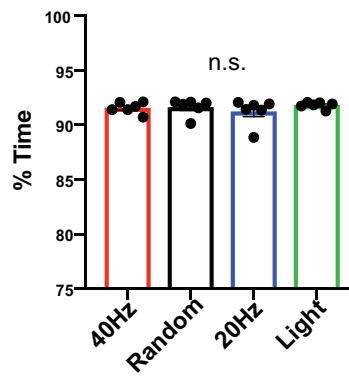
A Schematic of Sensory Stimulation



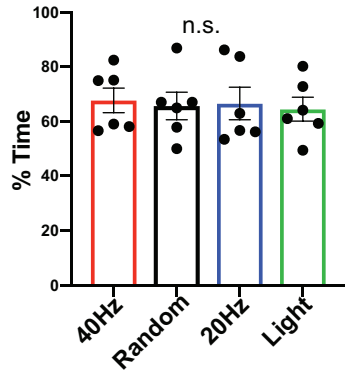
B Percent Time in Center



C Percent Time Active



D Percent Time in Back Half



E Total Distance Traveled

